Benefit of the MTG candidate Infra-Red Sounding mission to regional forecast
Report TN-3: Mid-term Review

Xiang-Yu Huang, Hongli Wang, Yongsheng Chen
National Center for Atmospheric Research, Colorado, USA

Xin Zhang
University of Hawaii, Honolulu, Hawaii, USA

Stephen A. Tjemkes, Rolf Stuhlmann
EUMETSAT, Darmstadt, Germany

ABSTRACT

Recent studies suggest that the accurate representation of the low-level water vapor is crucial for quantitative precipitation forecast. However, mesoscale observations of moisture usually are not available for most regions around the world. An Infra-Red Sounding (IRS) Mission on the Meteosat Third Generation (MTG) would provide high-resolution (in both space and time) temperature and water vapor information. Assimilating these observations into a mesoscale model is expected to improve skills in regional weather forecast. To evaluate such potentials, quantitative analyses of the added values of the IRS candidate mission for regional forecasts are performed by the means of Observing System Simulation Experiment (OSSE).

An OSSE of a series of convective storms occurred during 11 to 16 June 2002 has been conducted. A 5-day nature or "truth" run is generated with a high-resolution of 4-km using the Penn-State University/National Center for Atmospheric Research (NCAR) Mesoscale Model Version 5 (MM5). The conventional observations and MTG-IRS retrieved temperature and humidity profiles are simulated from the "truth". These observations are assimilated using the NCAR Weather Research and Forecasting (WRF) model and variational data assimilation system (WRF-Var) in cycling mode. Numerical forecasts initialized from the analyses are then carried out.

To calibrate the OSSE setup, data assimilation experiments using real conventional observations are conducted. Assimilating real or simulated conventional observations give similar error statistics in analyses and forecasts.

The results of data assimilation and forecast experiments show that, on average, the MTG retrieved profiles have positive impact on the analysis and forecast. The analysis reduces the errors in not only the temperature and the humidity, but also in the horizontal wind fields. The forecast skills of these variables are improved.

1. Introduction

Recent studies suggest that the accurate representation of the low-level water vapor is crucial for the quantitative precipitation forecast (e.g., Crook 1996, Xue et al. 2006). When realistic mesoscale details of the horizontal variations in moisture and surface moisture availability are included, pronounced improvements in forecast skills for convective events can be achieved (e.g., Koch et al. 1997; Parsons et al. 2000; Weckwerth 2000, 2004). However, mesoscale observations of moisture usually are not available for most regions around the world. EUMETSAT Delegations at the 46th PAC meeting commented that inclusion of an IRS sounding Mission on the Meteosat Third Generation (MTG) would be a new capability, when compared to the Meteosat Second Generation (MSG). IRS sounding Mission on MTG will provide high-resolution (in both space and time) temperature and water vapor information. Utilizing these observations in mesoscale model may improve skills in regional weather forecast. To evaluate such potentials, quantitative analyses of the added values of the IRS candidate mission for regional scale forecasts are performed by the means of OSSE.

This report summarizes the results of the OSSE of a series of convective storms occurred over USA during 11 to 16 June 2002. The synoptic situation is overviewed in section 2. The OSSE design and the numerical models and data assimilation system are introduced in section 3. Section 4 presents the results of one OSSE. Section 5 summaries the findings. The future works are also proposed.

2. Overview of selected cases

In this study, three convection cases occurred from 11 to 16 June 2002 during the International H2O Project (IHOP_2002, Wechwerth et al. 2004, Cai et al. 2006) are selected. Three cases include dryline, convective storms and severe mesoscale convective system (MCS). Figure 1 shows a series of visible satellite images for the selected three cases at the developing stage during which significant precipitations were observed.

On 11 June 2002, a dryline formed in the Oklahoma panhandle in the late afternoon. Although most numerical models predicted convection initiation, no deep convective storm formed near the dryline. Three other storms developed on this particular day in regions close to the IHOP_2002 intensive observing region (IOR). As shown by the upper left satellite image in Fig.1, a tornadic storm A was initiated near Russell, Kansas at 21UTC. Another small storm B formed around 22UTC along a stationary front. The third storm C was initiated along the roll boundary around 22UTC.

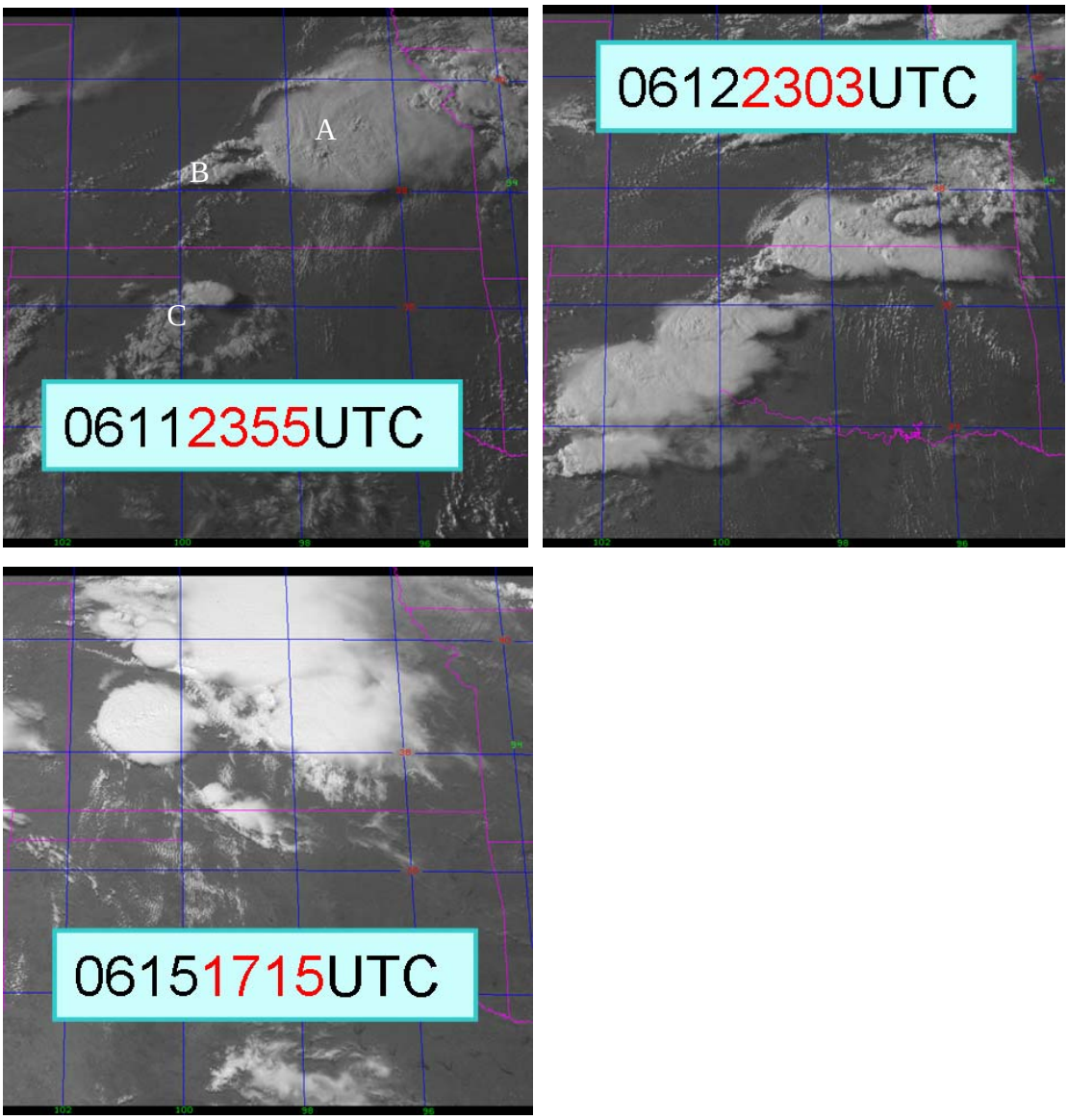

Fig.1. A series of visible satellite images valid at 2355UTC 11, 2303UTC 12, 1715UTC 15 June, 2002. Labels A, B, and C indicates three convective systems.

On 12 June 2002, a dryline led to the development of both shallow and deep cumulus clouds within the IOR, but these clouds failed to develop further into sustained cumulonimbus clouds. Approximately 40 km east of the IOR, severe convection was initiated, which is shown in the upper right panel of Fig.1.

The 15-16 June case is the severe mesoscale convective system (MCS) occurred over the U.S. central and southern plains in the late afternoon 15 June 2002. The lower panel of

Fig.1 shows that a large developing severe MCS was located from the northern Texas panhandle eastward across northern Oklahoma and southern Kansas. The MCS produced severe weather, including a few tornadoes, in southern Kansas, and a swath of wind damage reports through central Oklahoma southward and central Texas as it propagated southeastward.

These cases provide a good dataset for examining the differences between the numerical model prediction and what actually happened. Currently, the MTG-IRS retrieval algorithm can only provide temperature and humidity profiles over the clearly sky regions. It is interesting to see whether or not MTG-IRS retrievals can improve the analysis, and furthermore to improve the forecast skills of convective storms.

3. Observing system simulation experiment

In this study, the nature run and data assimilation experiments of an OSSE are performed using two different mesoscale models. Using different models has the advantage of avoiding that the forecasts follow the same model specific trajectory. The model errors can also be considered if the first model for the nature run is regarded as a perfect model. Another particular benefit of OSSE is that the forecast skills against the "truth" are available.

For the nature or "truth" run, we choose the 5^{th} generation Penn-State University/National Center for Atmospheric Research (NCAR) nonhydrostatic Mesoscale Model (MM5, Dudhia 1993). Conventional observations such as radiosonde and surface station observations are simulated from the nature run to provide the basic simulated observing system for the reference data assimilation experiment. Simulated MTG-IRS temperature and moisture profiles are then obtained from the nature run, either directly (perfect observations) or through MTG-IRS retrieval algorithm (Tjemkes, 2007).

The forecast model is the Weather Research and Forecasting (WRF) model (Michalakes, et al. 2001, Skamarock, et al. 2006). It produces the background for the data assimilation experiments and makes forecasts from the analyses. The simulated observations are assimilated using the WRF variational data assimilation system (WRF-Var) (Barker, et al. 2006). MTG-IRS retrieved profiles are assimilated in the presence of conventional data to access the their added values.

3.1 *Model setup*

MM5 is a limited-area, nonhydrostatic model, which is designed to simulate mesoscale atmospheric circulation. The model configuration chosen in this study employs 505×505

grid points with 4-km horizontal resolution and 35 vertical levels. The model top is at 50 hPa. The domain covers the central United State continent (Fig.2). The Medium Range Forecast boundary layer scheme (Hong and Pan 1996) and Reisener microphysics scheme (Reisener et al. 1998) are used. No cumulus parameterization scheme is used.

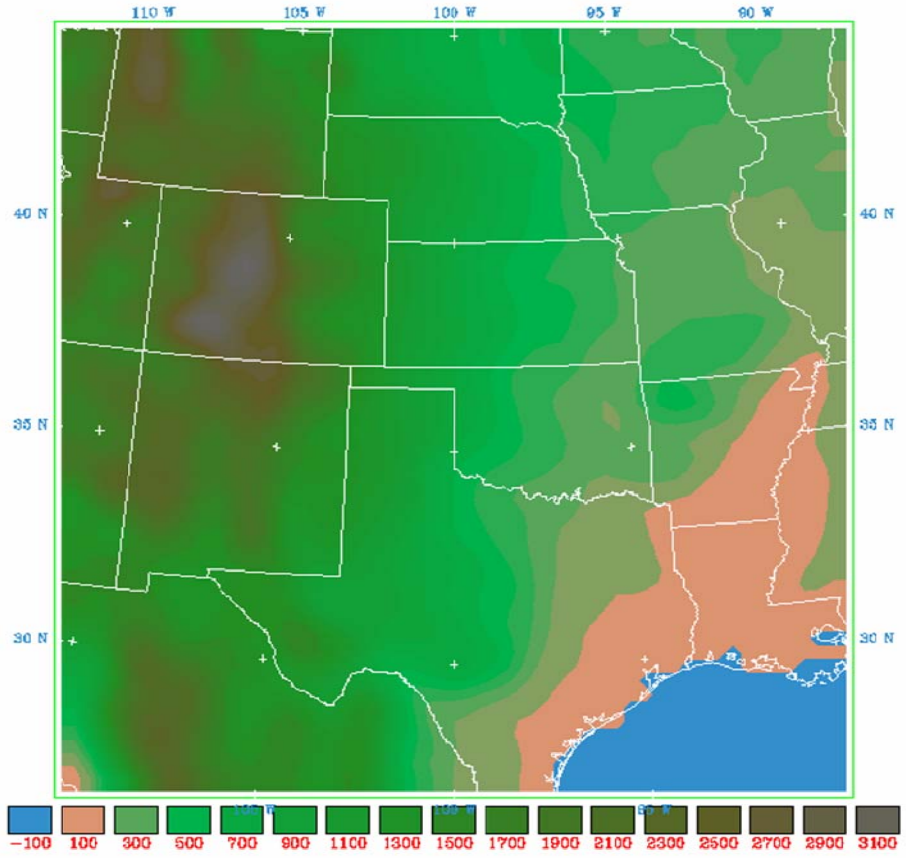

Fig.2 Model domain for both MM5 and WRF.

The WRF model is the next generation mesoscale model designed for cloud and mesoscale applications over a limited area (Michalakes et al. 2001, Skamarock, et al. 2006). The physics packages chosen for this study include the Noah land surface model (Chen and Dudhia 2001) and the Lin microphysics scheme (Lin et al. 1983, Chen and Sun 2002). The WRF model covers the same domain as MM5. For the planned high resolution experiments, the same resolution of 4 km and 505x505 grid points will be used. In this report, however, only 12-km resolution (172x172 grid points) experiments are presented. For the 12-km experiments, the Grell-Devenyi (2002) scheme is used for cumulus parameterization.

The WRF-Var developed at NCAR is a unified (global/regional, multi-model, 3/4DVAR) model-space variational data assimilation system (Barker, et al. 2006). A wide range of

observation types including conventional observations, radar, satellite radiances, etc., can be assimilated in WRF-Var. Only the 3-dimensional component of WRF-Var is used in this study. The 4-dimensional component of WRF-Var (4D-Var, Huang, et al. 2007b) may also be used at the later stage of this project.

3.2 ***Experiment design***

The nature run is produced using MM5. The model is initialized at 1200 UTC 11 June 2002 and run for 5 days. The initial and boundary conditions are interpolated from the National Center for Environment Prediction (NCEP) Eta model 40-km analyses. [Note the nature run configuration is different to that used in the preliminary report (Huang et al. 2007a).] The model state is saved hourly and then used as the truth from which the observations will be simulated. The conventional upper air and surface observations are extracted at the realistic synoptic time and station locations with observational errors added. The MTG-IRS temperature and moisture profile retrievals are simulated hourly using the true state. The observation errors for MTG-IRS temperature and moisture are specified as the sounding observations (1K for temperature and ~10-15% for moisture in terms of relative humidity).

We have conducted a number of data assimilation and forecast experiments. Nine experiments as listed in Table 1 and illustrated in Fig. 3 are presented in this report. These experiments shall provide reasonable assessments of the delta impact of the MTG-IRS retrievals. Note that in all the control and assimilations experiments list here, the WRF model is initialized from the 1-degree resolution NCEP Global Forecast System (GFS) 6-hourly analysis but not the ETA 40-km analysis.

The control run is firstly performed without data assimilation. In the control experiment, the WRF model is initialized from the GFS analysis at 12 UTC 11 June 2002, and integrated for 5 days. Its 6-h forecast valid at 1800 UTC 11 June 2002 serves as the background (BG) for the first cycle of other data assimilation experiments. This run is used as the basis for the comparison against the reference experiment with simulated conventional observations, to be discussed next.

Table 1. Lists of experiments

Experiment name	Cycling period	resolution	Initial condition and assimilated data
Nature	No	4 km	ETA 40 Km analysis
Control	No	12 km	GFS analysis
MOP	6 h	12 km	Background (BG) + simulated conventional observations
OP	6 h	12 km	Background (BG) + (real) conventional observations
MOP-RPq-6hc	6 h	12 km	Background (BG) + MOP +Retrieved profiles (q)
MOP-RPtq-6hc	6 h	12 km	Background (BG) + MOP +Retrieved profiles (T,q)
MOP-RPq-3hc	3 h	12 km	Background (BG) + MOP +Retrieved profiles (q)
MOP-RPtq-3hc	3 h	12 km	Background (BG) + MOP +Retrieved profiles (T,q)
MOP-RPq-1hc	1 h	12 km	Background (BG) + MOP +Retrieved profiles (q)
MOP-PRPq-6hc	6 h	12 km	Background (BG) + MOP +Perfect Retrieved profiles (q)

The data assimilation experiments here are different from those described in the preliminary report (Huang, et al. 2007a). Here, the delta impact of MTG-IRS retrievals is tested in a cycling data assimilation and forecast mode. In a cycling mode, a previous forecast is used as the first guess for the current analysis.

The reference experiment is MOP, in which only simulated conventional observations are assimilated. This experiment will be used as a reference for all MTG-IRS data impact experiments. To validate the performance of our data assimilation system for the designed OSSE, we also conducted an experiment, OP, in which the real conventional observations are assimilated.

To assess the added value of the retrieved MTG-IRS temperature and moisture profiles all data assimilation experiments have the simulated conventional observations included. In the experiments MOP-RP, added value of retrieved profiles (RP) is tested directly. For example, in the experiment MOP-RPq-6hc, only the MTG-IRS humidity profiles are assimilated in addition to the simulated conventional data every 6 hours, while the experiment MOP-RPtq-6hc has both temperature and humidity profiles assimilated. The experiment MOP-RPtq-3hc (MOP-RPq-3hc) is same as MOP-RPtq-3hc (MOP-RPq-6hc) except the assimilation cycling period is 3 hours. An hourly cycling experiment MOP-RPq-1hc is also carried out.

The experiment MOP-PRPq-6hc is similar to MOP-RPq-6hc except that the true humidity profiles collocated with RP are assimilated. This experiment is designed to assess the maximum potential impact of the retrieved humidity profiles by assuming the retrievals have no errors.

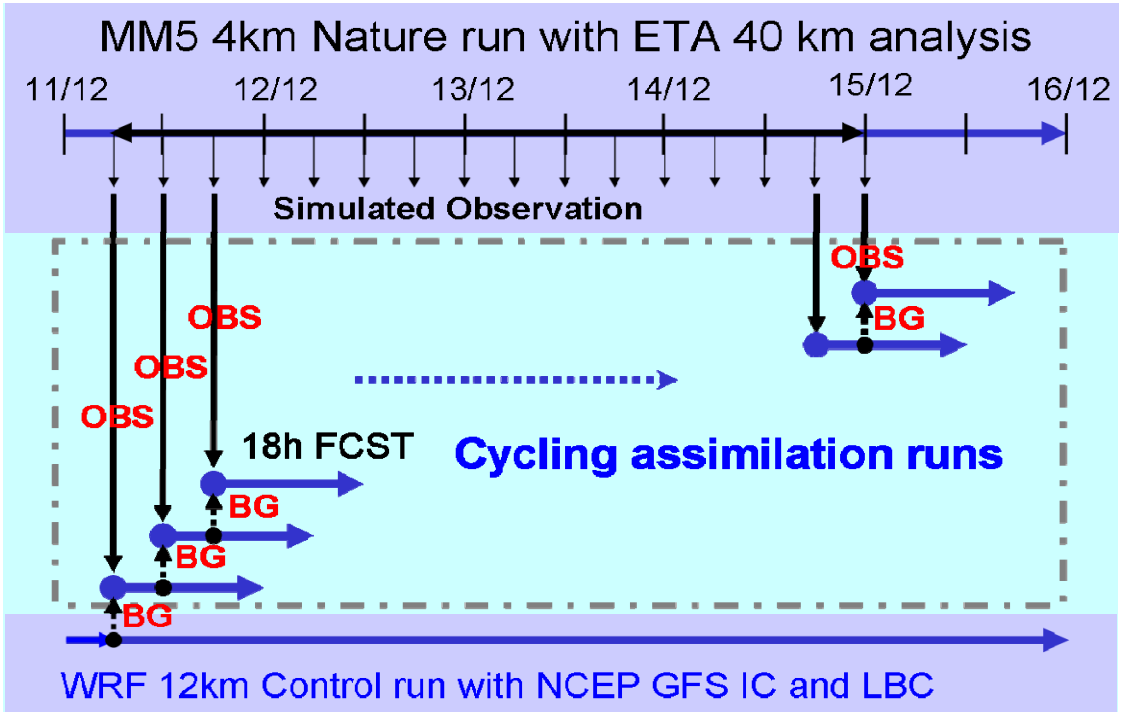

Fig.3. Flow chart of three experiments

3.3 ***Verification***

The impacts of MTG-IRS data on the regional scale analysis and forecast are assessed in terms of root-mean-square (RMS) error and bias between an experiment and the "truth".

Comparisons of the precipitation forecasts among various experiments and the "truth" are also shown in the report. For verification at a given threshold, the forecasts and observations, were categorized into two categories, rain or no rain, and the forecast–observation pairs accumulated into 2 by 2 contingency tables according to the four possible outcomes: (a) hits (rain forecast and rain observed), (b) misses (rain observed but not forecast), (c) false alarms (rain forecast but not observed), and (d) correct negatives.

The equitable threat score (ETS) of rainfall is computed as follows:

$$ETS = (hits - hits_{random}) / (hits + misses + false\ alarms - hits_{random})$$

Here $hits_{random}$ is:

$$hits_{random}=((hits + misses) \times (hits + false\ alarms))/(hits + misses + false\ alarms + correct\ negatives)$$

The frequency BIAS is the ratio of the number of rain forecasts to the number of rain observations:

$$BIAS = (hits + false\ alarms)/(hits + misses)$$

4. Results

4.1 *The nature run*

A 5-day nature run covering the selected three IHOP_2002 convective events is completed first. Figure 4 compares the 6-h accumulated precipitation of the nature run to the observations. The rainfall observations used here are the Stage IV analyses, which are based on the multi-sensor hourly/6-hourly 'Stage III' analyses on local 4km polar-stereographic grids produced by the 12 River Forecast Centers (RFCs) for CONUS. For more description, the reader is referred to http://data.eol.ucar.edu/codiac/dss/id=21.093. In general, MM5 nature run simulates well the position of the three rainfall events. The nature run slightly over-estimates the precipitation for the first case and under-estimates the precipitation for the third case.

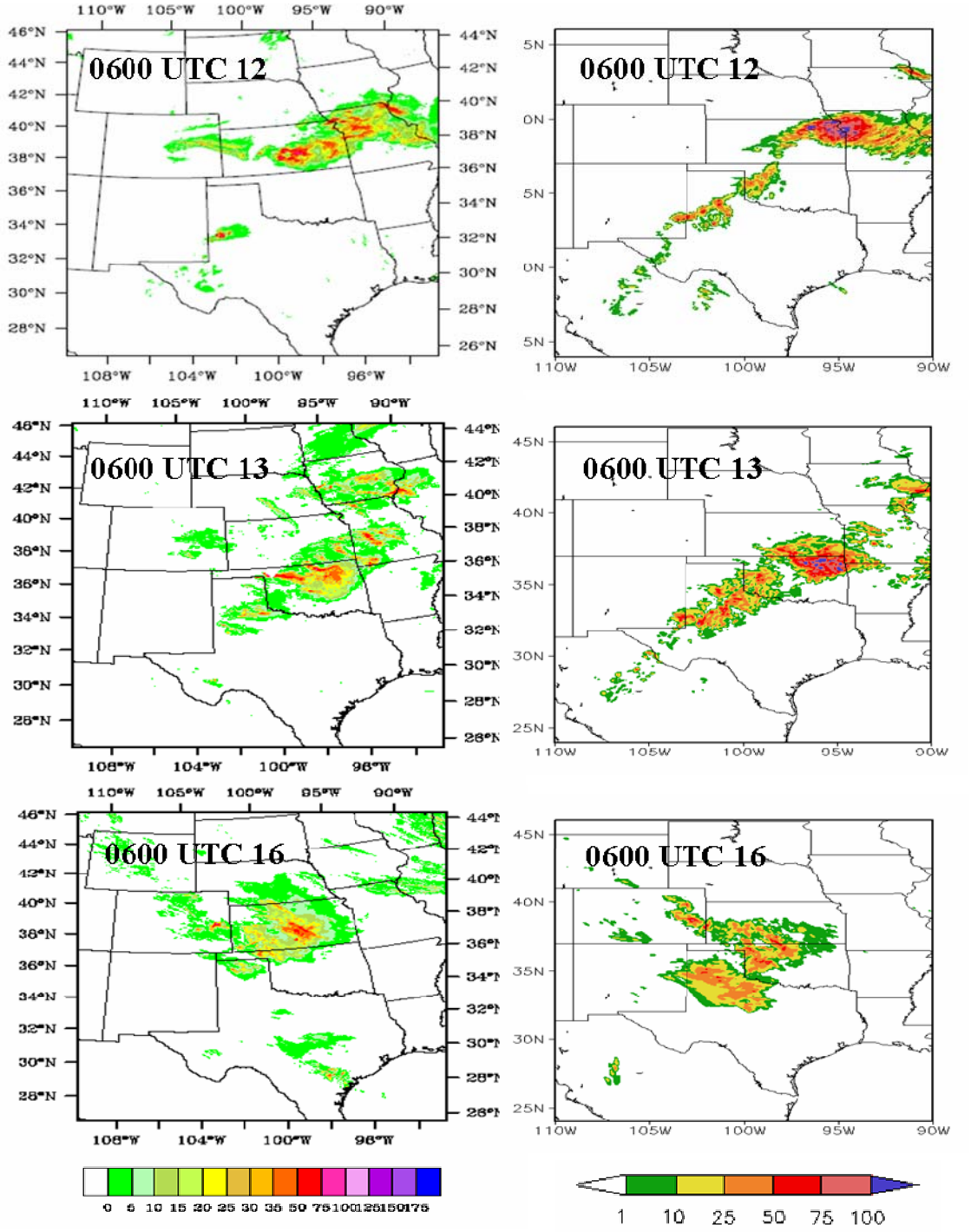

Fig.4. 6-h accumulated precipitation in the observation (left) and in the nature run (right) valid at 0600 UTC 12 (top), 0600 UTC 13 (middle) and 0600 UTC 16 (bottom) June 2002. Note the color scales and map projections are different between the observation and the simulation.

4.2 ***Simulated observations***

Given the true state, simulated observations can be generated. The positions and observation types of the real upper-air and surface observations are obtained from the NCEP Automated Data Processing upper-air (ADPUPA) and surface (ADPSFC) observations. The ADPUPA includes radiosondes and pibals launched at the upper air stations and ships. The ADPSFC data includes SYNOP, METAR, AWOS and ASOS land surface station report types (see http://dss.ucar.edu/datasets/ds353.4/, http://dss.ucar.edu/datasets/ds464.0/ for detailed description of ADPUPA and ADPSFC data). The observation operators in WRF-3Dvar are employed to produce simulated conventional observations from the MM5 Nature run. The temperature, dew point temperature and horizontal winds are all simulated. The true simulated observations are obtained first, then the realistic observation errors with Gaussian distributions are added.

The temperature and water vapor mixing ratio profiles over clear air region are retrieved using MTG-IRS sounding algorithm (Tjemkes, 2007). The retrieval algorithm has been improved over the course of this project. The most recent retrieval data reduces errors in temperature and moisture significantly, which lead to many improvements in the analysis and forecast.

The distributions of the simulated observations as well as the MTG-IRS retrievals are illustrated in Fig.5. The numbers of upper air observations vary from cycle to cycle, more at 00 UTC/12 UTC and less at 06UTC/18UTC. For surface observations, the numbers remain almost unchanged throughout the 6-h cycles. There are very little changes in the positions of the conventional data. However, the numbers and positions of the MTG-IRS retrievals can change a lot due to weather conditions. (Note here as we treat MTG-IRS profiles as radiosondes the RP distributions shown at the bottom of the figure also include ADPUPA.)

To compare the truth and the retrievals, Figs.6 and 7 show the temperature distributions in the nature run and the latest retrievals at 850 hPa, valid at 18UTC 11 June 2002, and 18UTC 12 June 2002, respectively. The BIAS and RMS error are shown in Fig.8. In general, the retrievals faithfully represent the relatively large-scale patterns and some mesoscale details of the real temperature field, especially in the middle atmosphere. It is evident that the averaged retrieval errors vary in vertical direction. The maximum error in the retrievals is about 2 K, and the RMS error is about 1 K, which is comparable to the radiosonde observations. The retrievals are more accurate in the middle levels from 600 to 200 hPa.

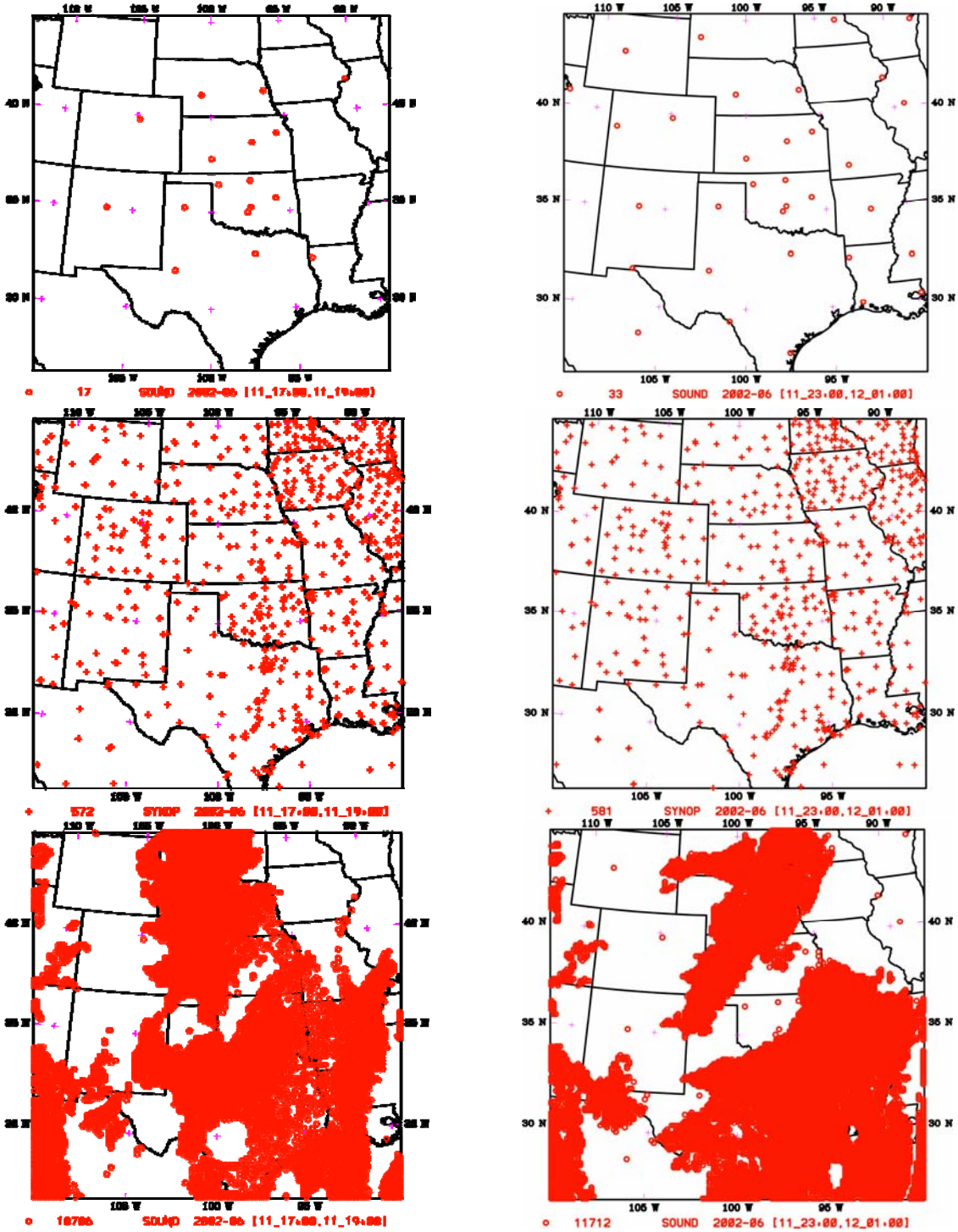

Fig.5. The distribution of simulated ADPUPA (top), ADPSFC (middle) and RP (bottom) data at 1800 UTC 11 June 2002 (left) and 0000 UTC 12 June 2002 (right). For ADPUPA and ADPSFC, observations within +/- 1-hour are included.

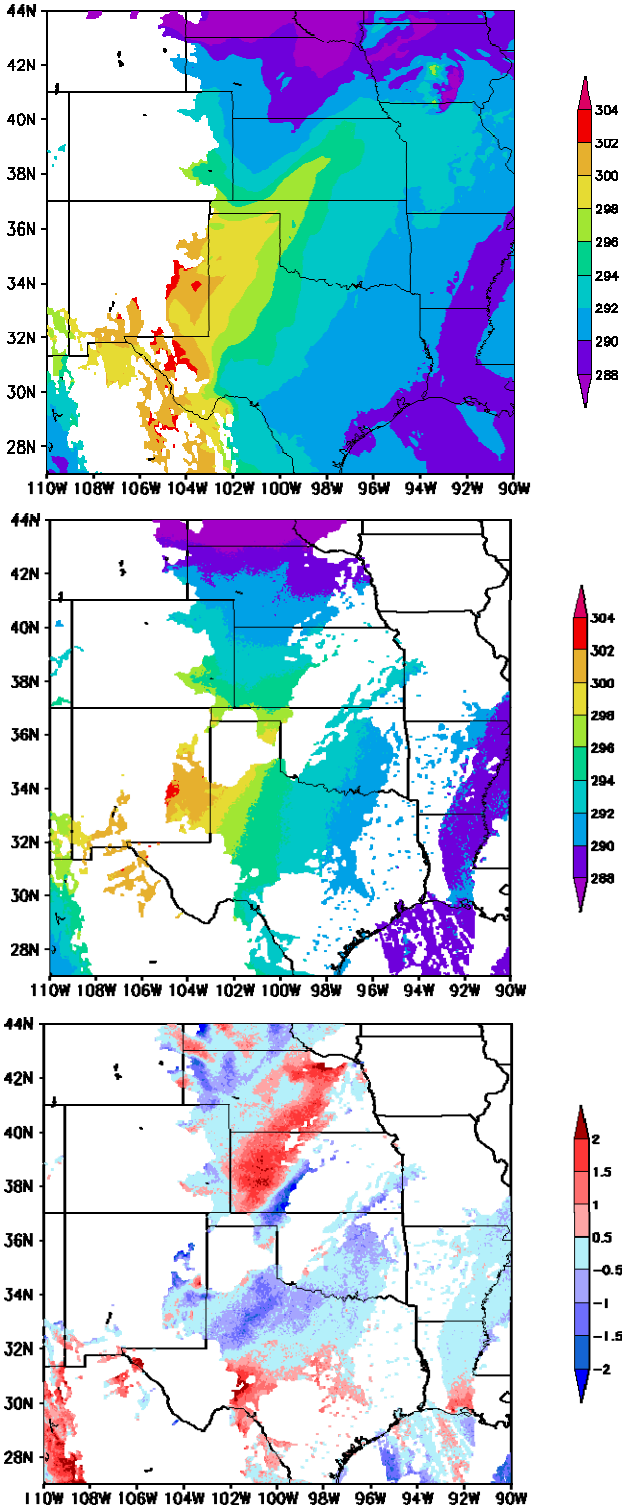

Fig.6. Temperature (K) valid at 18UTC 11 June 2002 of the truth (top), the retrievals (middle) and the difference (bottom) on 850 hPa. The white regions have missing values.

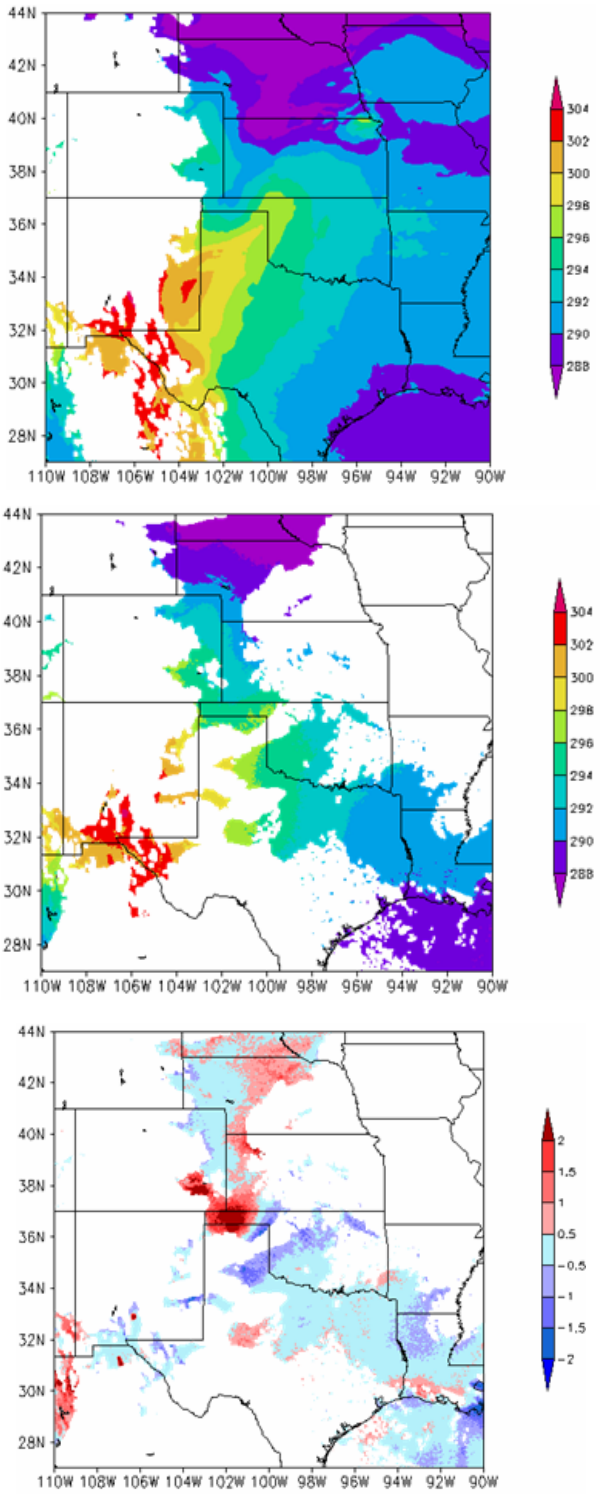

Fig.7. Temperature (K) valid at 18UTC 12 June 2002 of the truth (top), the retrievals (middle) and the difference (bottom) on 850 hPa. The white regions have missing values.

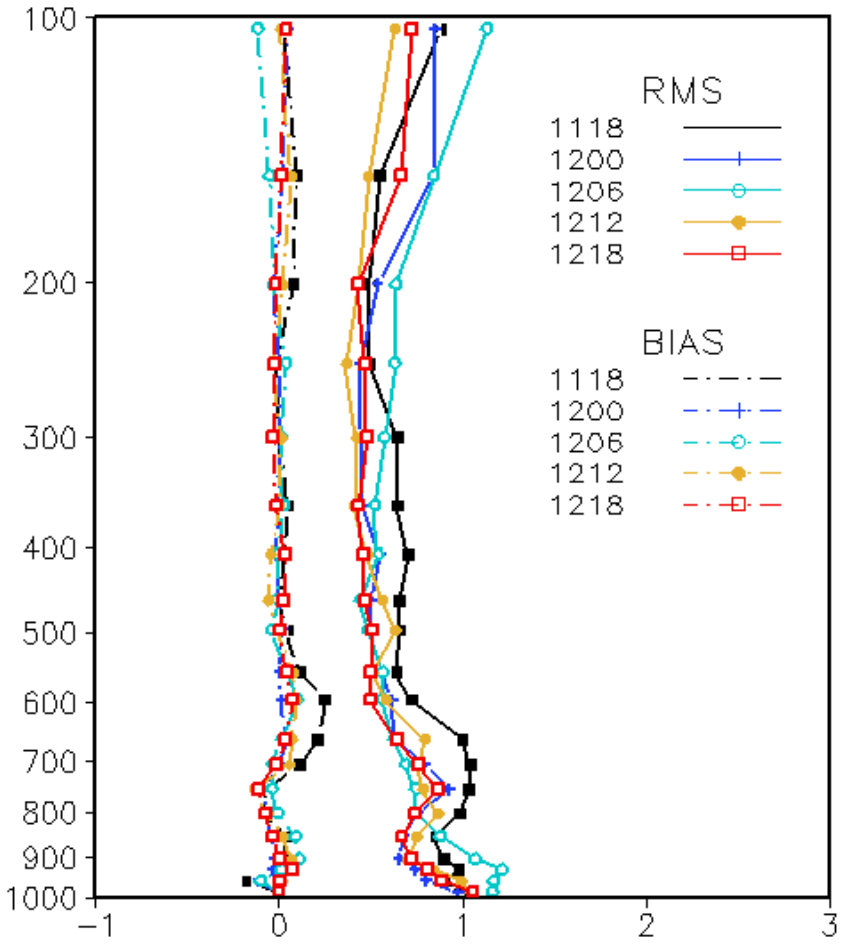

Fig.8. BIAS and RMS error of the retrieved profiles of T (K) valid at different times. Legends show day and hour.

Figures 9, 10 and 11 show retrieved moisture profiles agreeing decently with the true values. The maximum error is about 2 g/kg. Comparing to the earlier retrieval data, the bias is much reduced. The RMS error is improved in levels above 800 hPa. The retrieved water vapor mixing ratio has maximum RMS errors near the surface, and dry bias below 800 hPa.

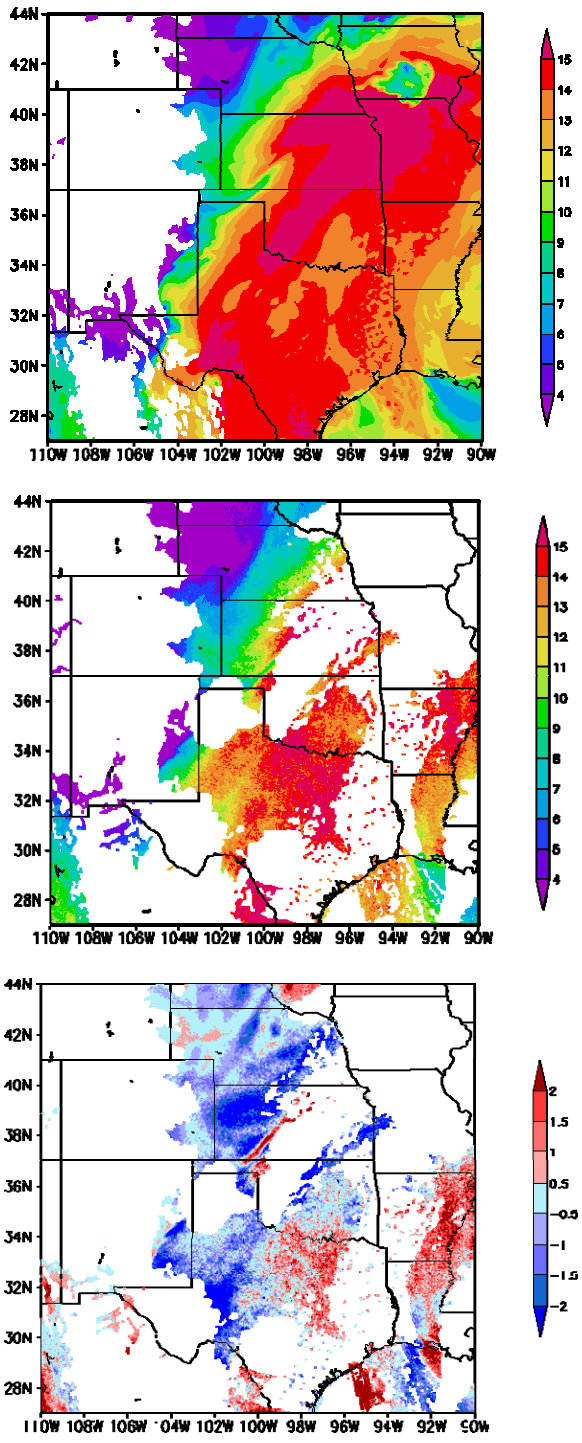

Fig.9. Water vapor mixing ratio (g/kg) valid at 18UTC 11 June 2002 of the truth (top), the retrievals (middle) and the difference (bottom) on 850 hPa. The white regions have missing values.

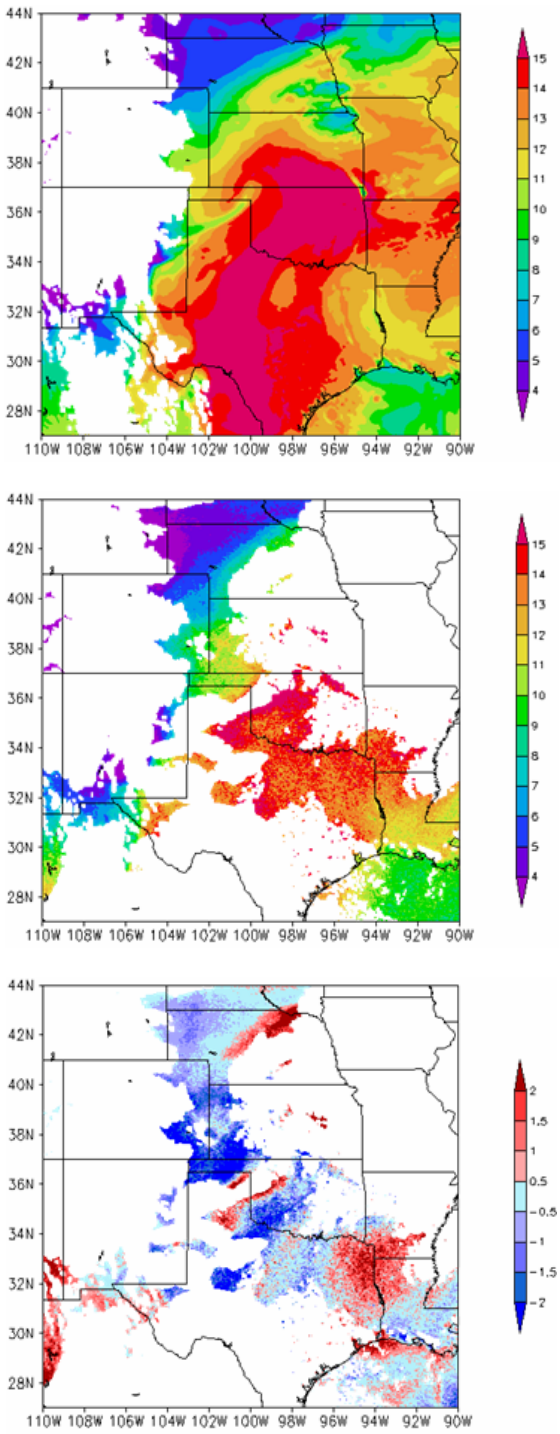

Fig.10. Water vapor mixing ratio (g/kg) valid at 18UTC 12 June 2002 of the truth (top), the retrievals (middle) and the difference (bottom) on 850 hPa. The white regions have missing values.

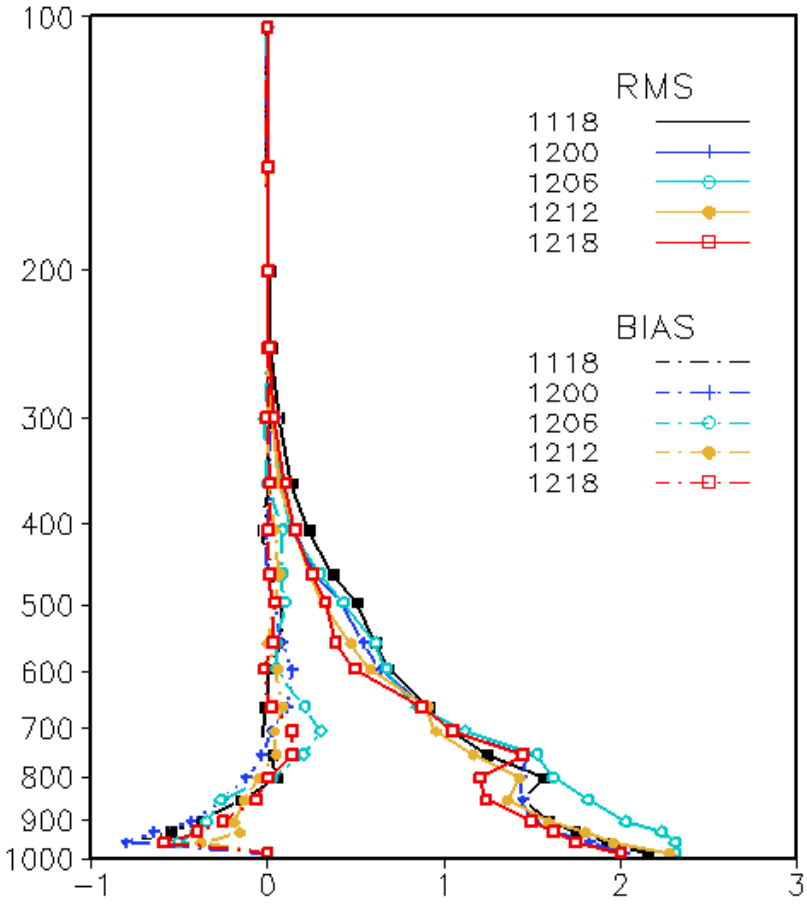

Fig.11. BIAS and RMS error of the retrieved profiles of water vapor mixing ratio (g/kg), valid at different times. Legends show day and hour.

4.3 ***Background error covariance***

Background error covariance (BE) plays an important role in the 3D-Var system. In this report, the National Meteorological Center (NMC) method (Parrish and Derber 1992) is used to generate the BE suitable for our experiments using the utility packages in WRF-Var system. A set of cold start forecasts are initiated from NCEP GFS analysis at 0000 UTC and 1200 UTC every day from 5 June 2002 to 19 June 2002. The differences of 24-h and 12-h forecasts are used to derive BE. The model domain has 172x172x35 grids with 12-km resolution which covers the same domain as the MM5 nature run.

The generated BE is tested in a number of single observation experiments. Figure 12 gives one example of the single observation experiments. A pseudo observation of

temperature with the value 2 K higher than the first guess field and 1 K error is specified at the centre of the lowest model level. The analysis produces a maximum of 1 K potential temperature increment. The increments in *v* show a cyclonic circulation at low level and anti-cyclonic circulation in the middle level. The maximum u and v increment is about 0.25 m/s. The results demonstrate that the wind will be changed through the background error covariance even though we only assimilated retrieved MTG-IRS temperature profiles. It also suggests that wind observations from other observation platforms will be helpful to provide constraints on the wind analysis.

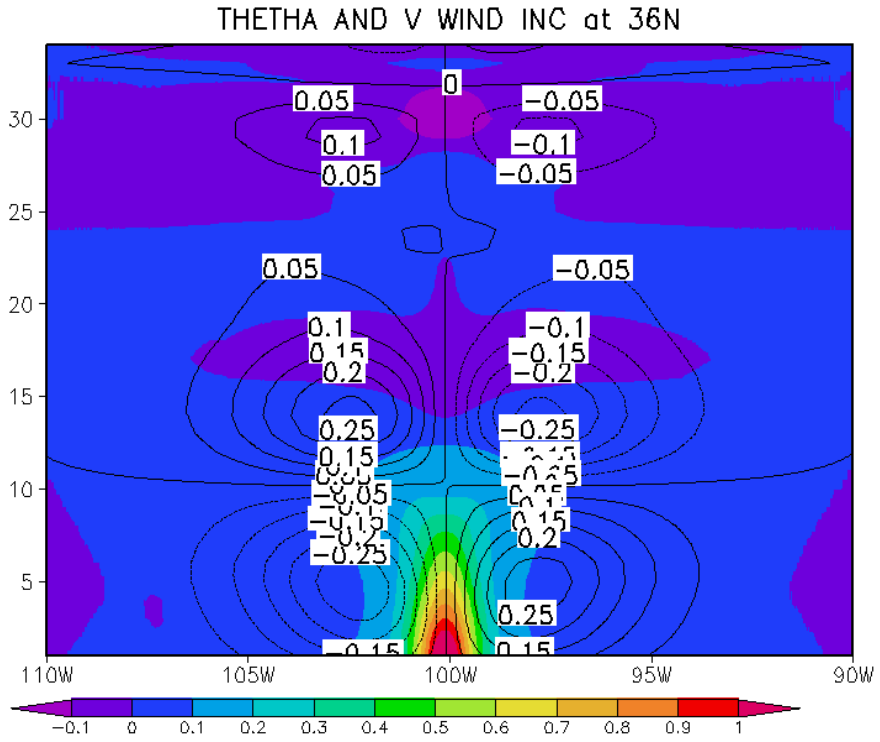

Fig.12. Potential temperature (shaded) and *v* (contours) increments due to a single temperature observation at the lowest level in the middle of the model domain.

4.4 ***Calibration experiments***

To validate the performance of our data assimilation system for the designed OSSE, we first conducted a pair of calibration experiments OP and MOP to compare the impacts from assimilating real or simulated conventional observations. The calibration experiments are carried out at 12-km resolution with 172×172 grids.

Figures 13 to 16 show the BIAS and RMS errors for temperature, water vapor mixing ratio, *u*-wind and *v*-wind components of analyses and forecasts. Two sets of observations produce similar error statistics. It suggests that further results of the designed OSSE using simulated observations shall generate similar characteristics as the real data experiments.

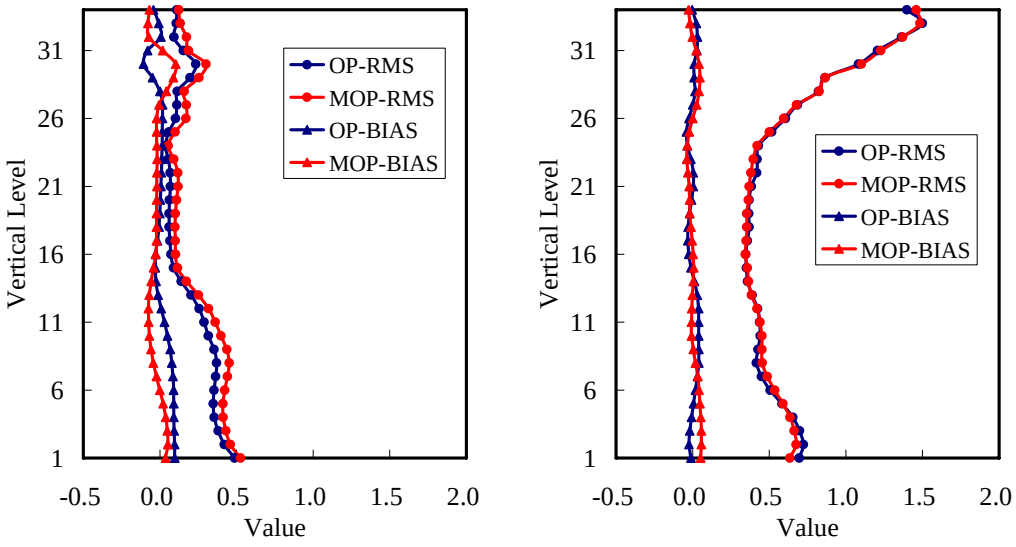

Fig.13. BIAS and RMS error in temperature (K) of a) analyses and b)18-h forecasts, averaged over 18UTC 11 June and 12UTC 15 June 2002.

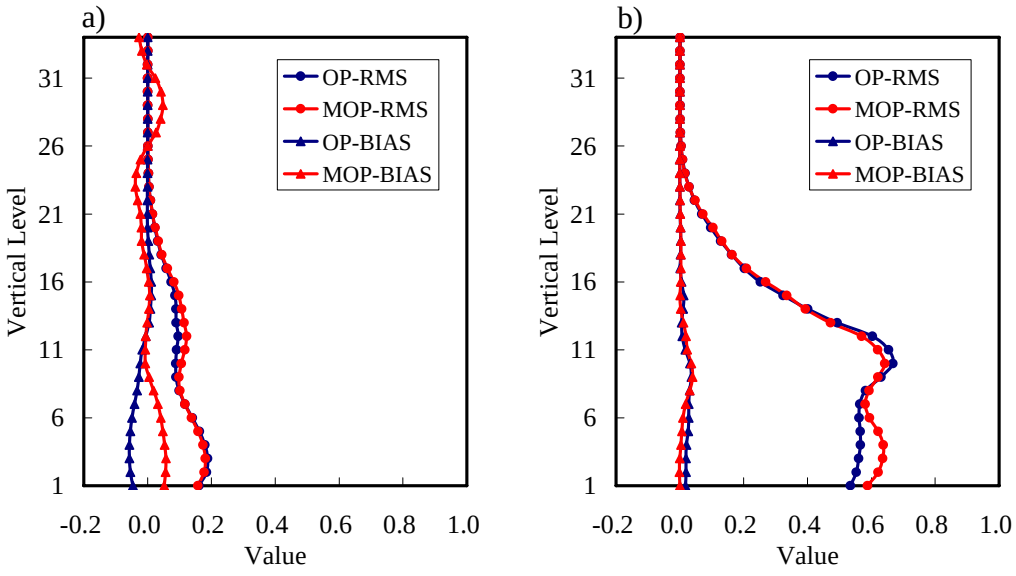

Fig.14. BIAS and RMS error in water vapor mixing ratio (g/kg) of a) analyses and b) 18-h forecasts, averaged over 18UTC 11 June and 12UTC 15 June 2002.

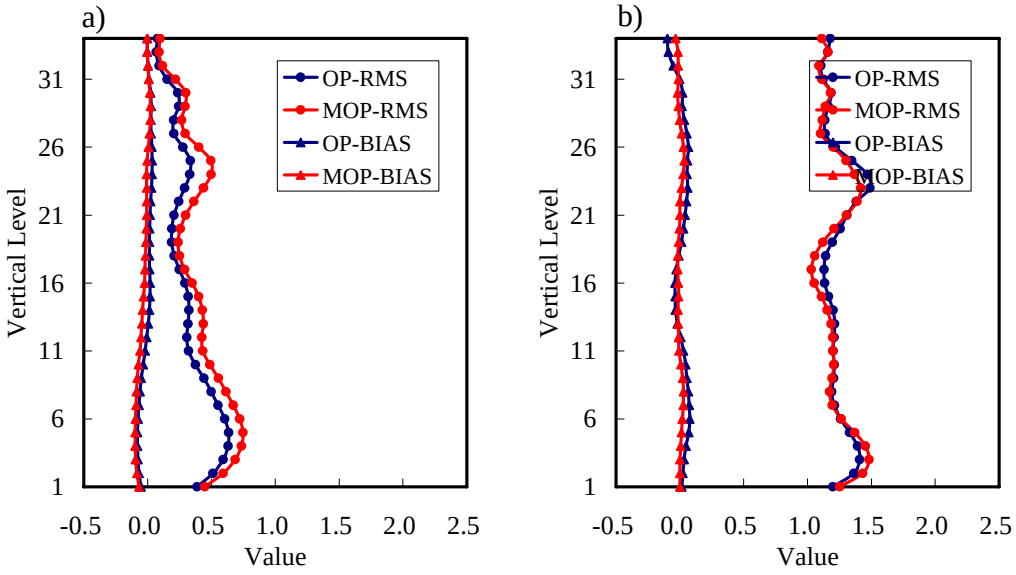

Fig.15. BIAS and RMS error in zonal wind component (m/s) of a) analyses and b) at 18-h forecasts, averaged over 18UTC 11 June and 12UTC 15 June 2002.

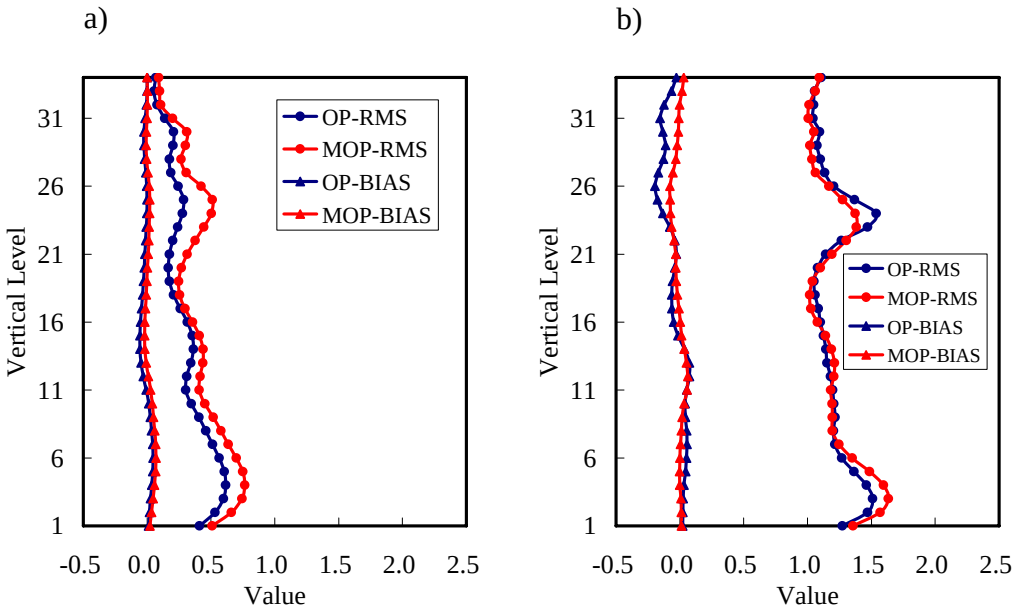

Fig.16. BIAS and RMS error in meridional wind component (m/s) of a) analyses and b) 18-h forecasts, averaged over 18UTC 11 June and 12UTC 15 June 2002.

4.5 ***Analysis and forecast in 6-hourly cycling experiments***

The WRF-Var analyses were performed in cycling mode starting from 1800 UTC 11 to 1200 UTC 14 June. The first two storm cases described in Section 2 occurred in this period. To better understand the impact of MTG-IRS retrieved profiles, three types of analysis differences are computed, 1) the results of assimilating conventional observations (MOP) minus the first guess; 2) the results of assimilating conventional observations and MTG-IRS retrievals (MOP-RPtq or MOP-RPq) minus the results of MOP; 3) the difference between the analysis and the "truth". As shown in Fig.5, the observation number of MTG-IRS retrieval profiles is much larger than that of the conventional observations in MOP. We expect that the MTG-IRS observations has larger impact on analysis in addition to MOP, and the analysis should be more accurate compared with assimilating of MOP if the MTG-IRS retrievals are of good quality.

Figures 17 to 20 give the analysis increments of the temperature (*T*), water vapor mixing ratio (*q*), and horizontal wind (*u* and *v*) at 850hPa in the experiments MOP ,the analysis differences between MOP-RPq-6hc and MOP experiments, between MOP-RPtq-6hc and MOP experiments, and between analysis and the "truth", respectively. Assimilating the MTG-IRS retrievals leads to significant adjustments in *T*, *q*, *u* and *v* fields. Assimilating moisture retrievals (MOP-RPq-6hc) has larger impacts on q analysis than assimilating both temperature and moisture retrieval profiles (MOP-RPtq-6hc). The maximum *q* increment is about 4 g/kg in the former, while larger adjustment in *u* is obtained in the latter.

Comparing Fig.17 d), e) and f), it is found that MTG-IRS observations help to improve the temperature analysis near the shore in Texas. In experiment MOP-RPtq-6hc, the temperature analysis is improved over Nebraska as well since the retrievals are accurate in the region (Fig.6), but degraded over Oklahoma due to the cold bias in RP in the surrounding area (Fig.6).

Figure 18 shows that the humidity analysis in MOP-RPq-6hc is degraded near Rocky Mountain in New Mexico and Texas due to the dry bias in the humidity retrieval in this region (cf. Fig.9). However, in MOP-RPtq-6hc, humidity analysis along Rocky Mountain is improved when both temperature and moisture retrievals are assimilated.

MTG-IRS retrievals have small impact on *v* analysis than on *u* analysis comparing Fig.20 a), b) and c) with Fig.21. In the Mop-RPq-6hc, *u* analysis near Nebraska and Kansas is improved, but in Mop-RPtq-6hc, the *u* analysis in this region is degraded. According to the relation between temperature and wind in background error matrix, the spurious cold temperature increment (Fig.17c) leads to a spurious anti-cyclonic circulation (Fig.19c).

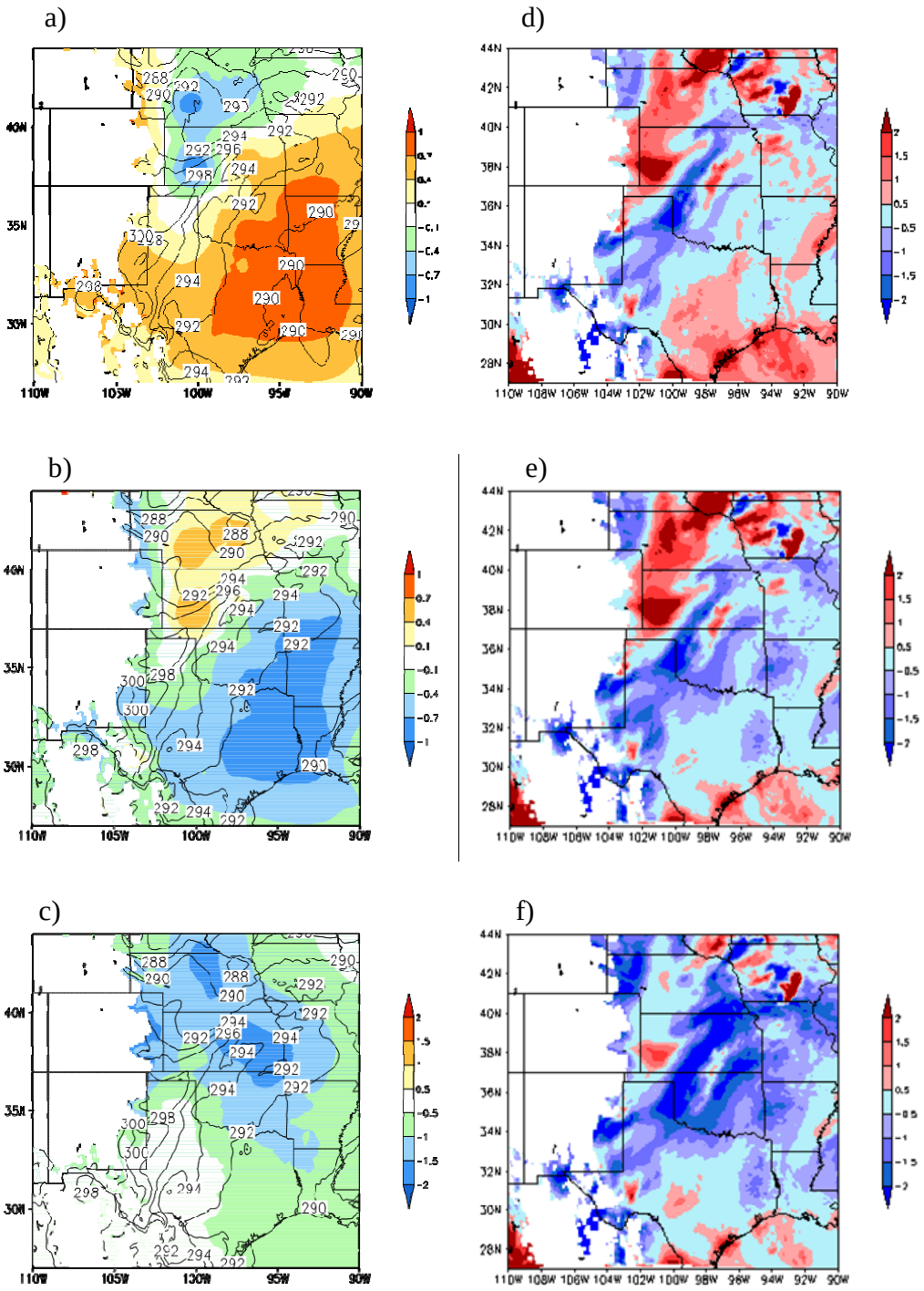

Fig.17. The difference (shaded) of the 850 hPa temperature *T* (unit: K) between (a) MOP and Control, (b) MOP-RPq-6hc and MOP, and (c) MOP-RPtq-6hc and MOP, d) MOP and "truth", (e) MOP-RPq-6hc and "truth", and (f) MOP-RPtq-6hc and "truth", valid at 1800 UTC 11 June. The contours show the temperature in a) MOP, b) MOP-RPq-6hc, and c) MOP-RPtq-6hc.

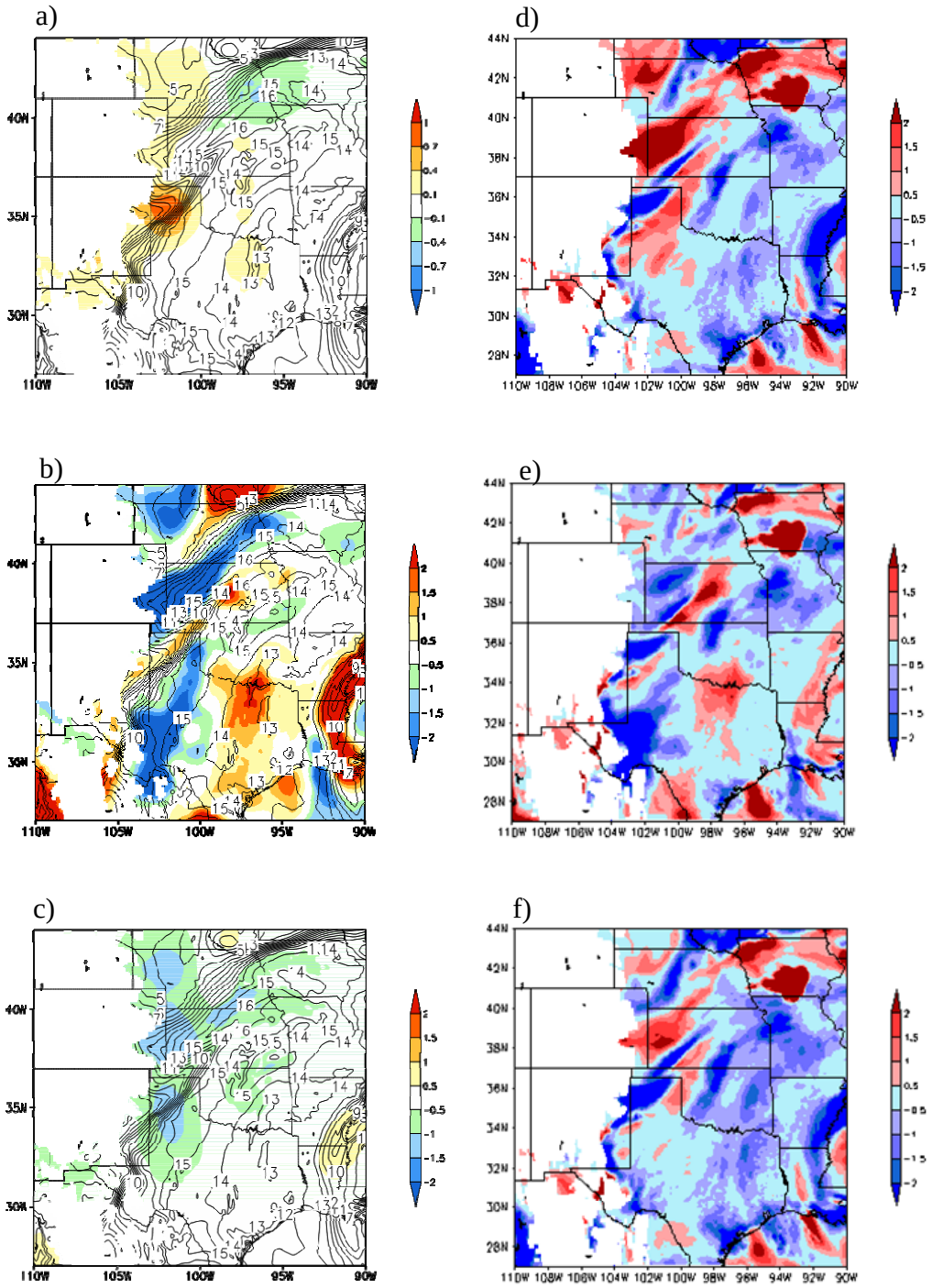

Fig.18. The difference (shaded) of the 850 hPa water vapor mixing ratio *q* (unit: g/kg) between (a) MOP and Control, (b) MOP-RPq-6hc and MOP, and (c) MOP-RPtq-6hc and MOP, d) MOP and "truth", (e) MOP-RPq-6hc and "truth", and (f) MOP-RPtq-6hc and "truth", valid at 1800 UTC 11 June. The contours show *q* in a) MOP, b) MOP-RPq-6hc, and c) MOP-RPtq-6hc.

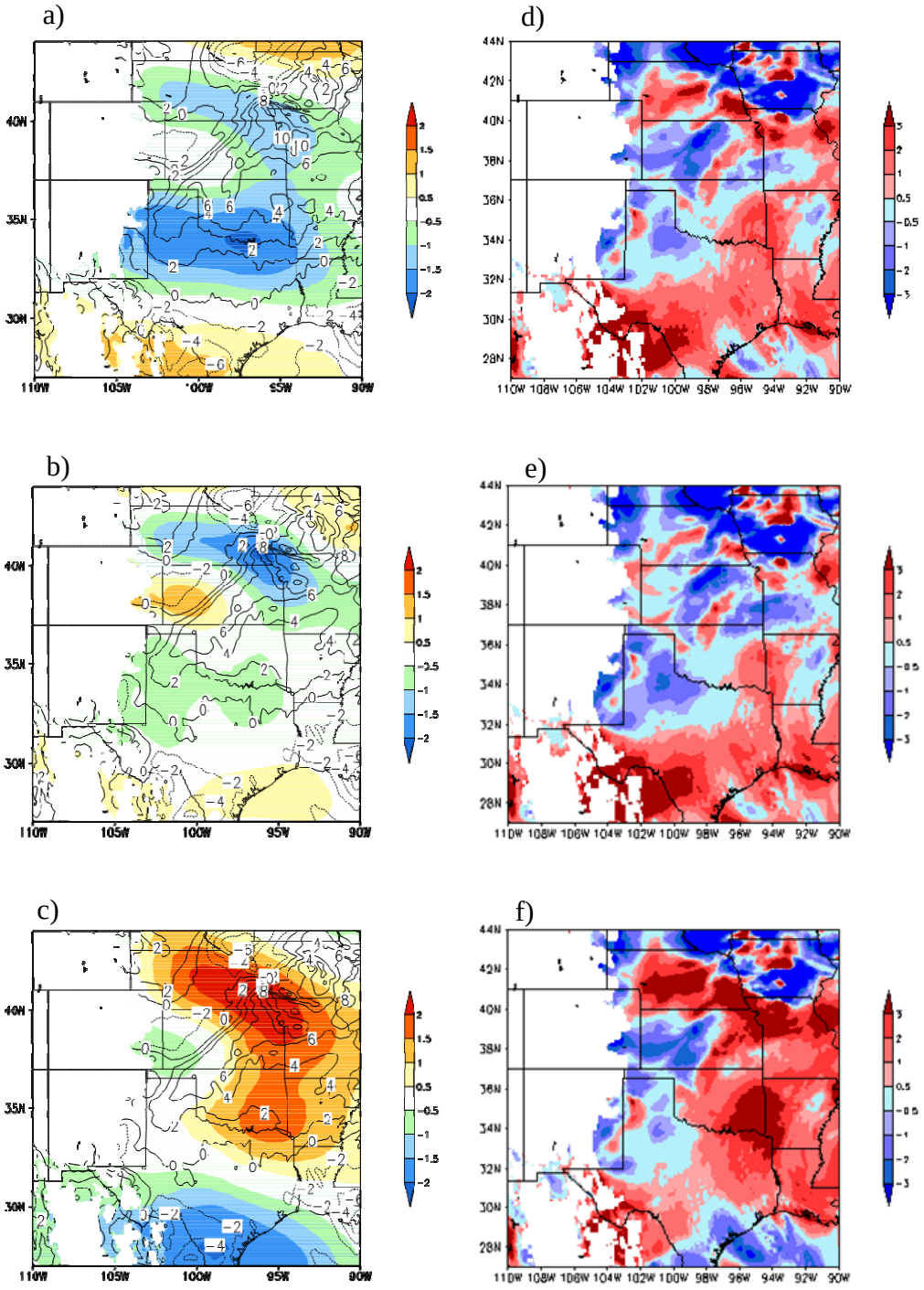

Fig.19. The difference (shaded) of the 850 hPa zonal wind component *u* (unit: m/s) between (a) MOP and Control, (b) MOP-RPq-6hc and MOP, and (c) MOP-RPtq-6hc and MOP, d) MOP and "truth", (e) MOP-RPq-6hc and "truth", and (f) MOP-RPtq-6hc and "truth", valid at 1800 UTC 11 June. The contours show *u* in a) MOP, b) MOP-RPq-6hc, and c) MOP-RPtq-6hc.

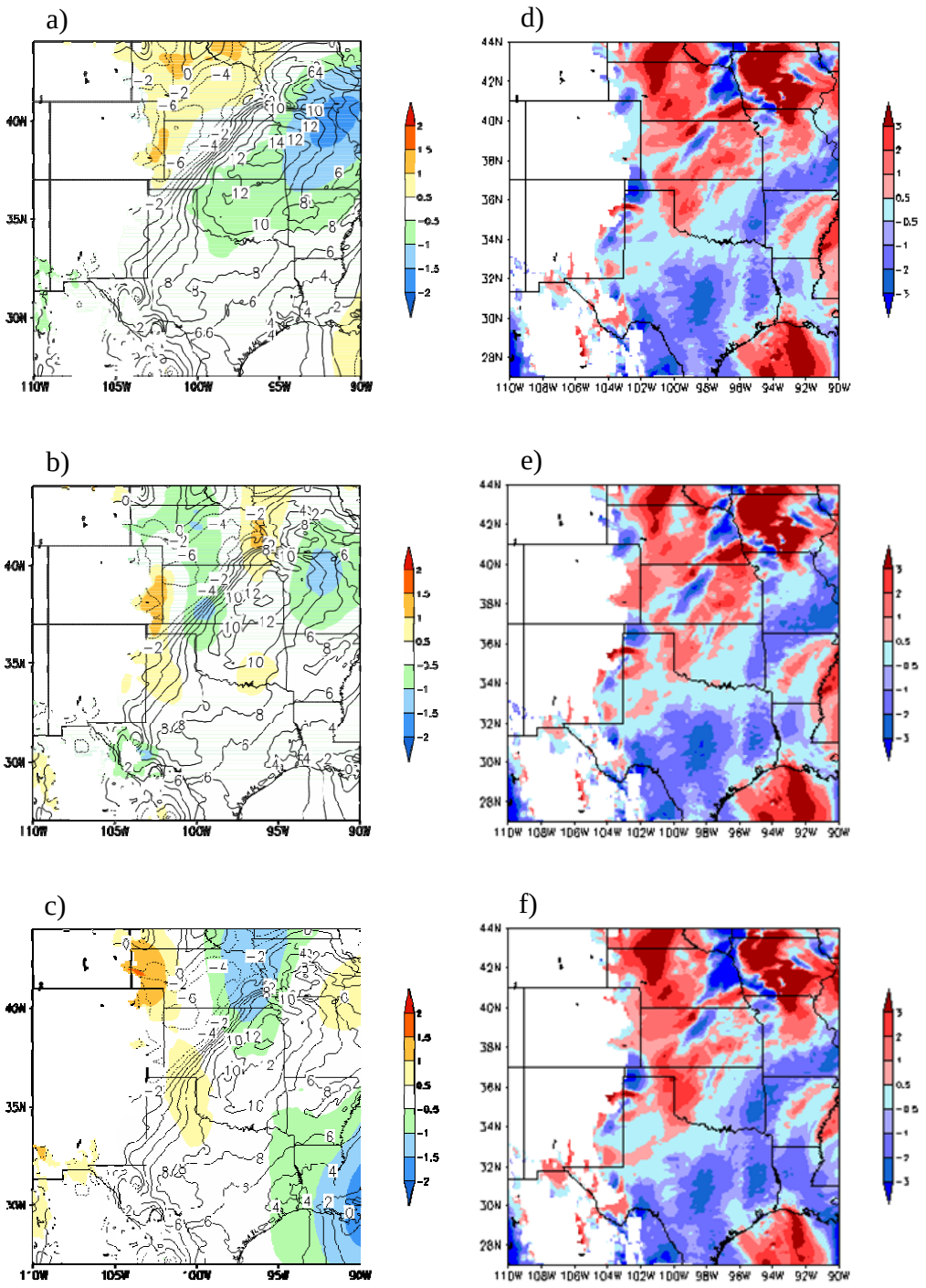

Fig.20. The difference (shaded) of the 850 hPa meridional wind component *v* (unit: m/s) between a) MOP and Control, b) MOP-RPq-6hc and MOP, and c) MOP-RPtq-6hc and MOP, d) MOP and "truth", (e) MOP-RPq-6hc and "truth", and (f) MOP-RPtq-6hc and "truth", valid at 1800 UTC 11 June. The contours show *v* in a) MOP, b) MOP-RPq-6hc, and c) MOP-RPtq-6hc.

Using the nature run as the “truth”, the RMS errors of the analysis and the forecast are computed. Figure 21 depicts the RMS errors for all experiments at the analysis time. As we expected, assimilating the simulated observations (MOP) and the MTG-IRS retrievals significantly reduces the analysis errors compared to the control experiment. Comparing MOP-RPtq-6hc and MOP-RPq-6hc, assimilating both temperature and moisture retrievals gives the better temperature analyses, but degrades the *u* and *v* analyses. Similar improvements in moisture analyses of both experiments are obtained due to weak correlations between *T* and *q* in BE.

The maximum potential impact of moisture retrieval on analyses can been found in MOP-PRPq-6hc in which the MTG-IRS moisture retrievals are replaced by nature runs values. Assimilating the accurate moisture observations produces the best analyses of *u*, *v*, and *q* of all the cycling experiments. However, it is clear that RMS errors of *T*, *u* and *v* analyses in MOP-RPq-6hc are similar to those of MOP-PRPq-6hc. Given the present BE, when the quality of the *q* retrievals is improved, only the *q* analysis has large room to be improved.

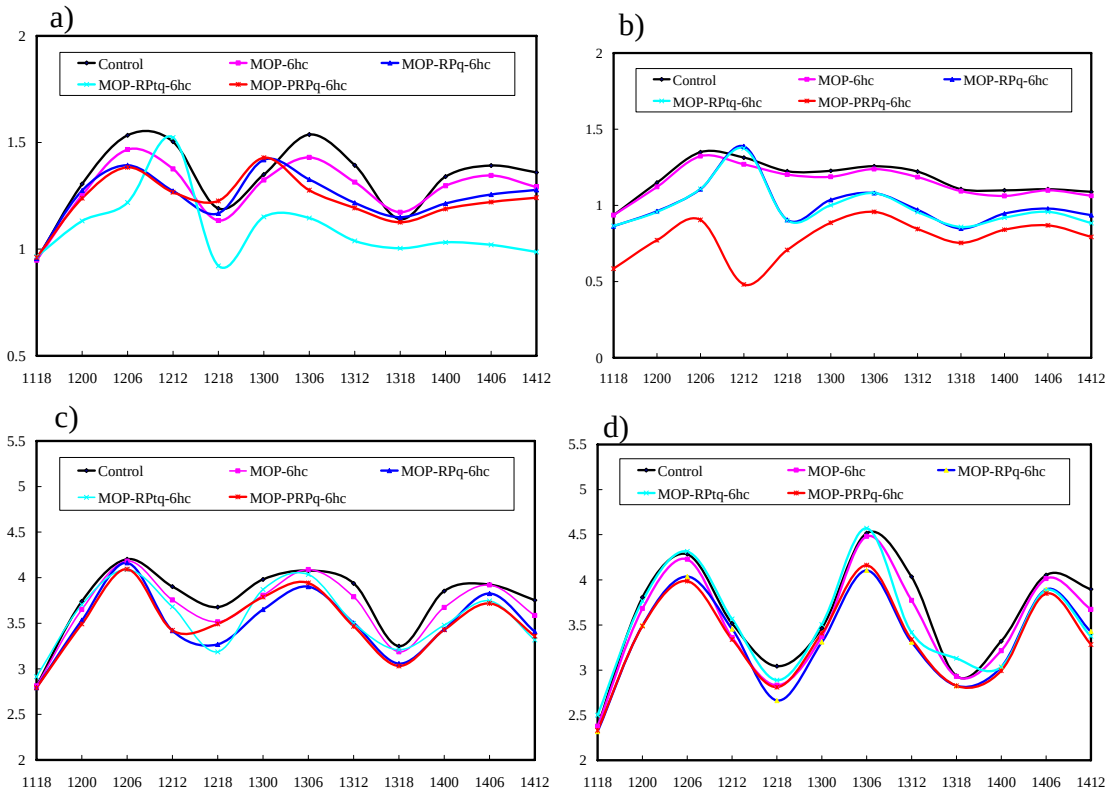

Fig. 21. RMS error, averaged over the model domain, at different analysis time in 6-hourly cycling experiments for a) temperature *T* (K), b) water vapor mixing ratio *q* (g/kg), c) *u* (m/s), and *v* (m/s).

In each 6-hourly cycling experiment, there are 16 analyses and forecasts during the cycling period. Figure 22 shows that assimilating simulated conventional observations (MOP) improves the forecasts over the control run (without any observation). When the MTG-IRS retrievals are assimilated, all the analyses and forecasts are, on average, improved. When the accurate humidity observations are assimilated with conventional observations, the moisture analysis and forecast are improved significantly, but no obvious impacts on *T*, *u* and *v* analyses and forecasts are obtained.

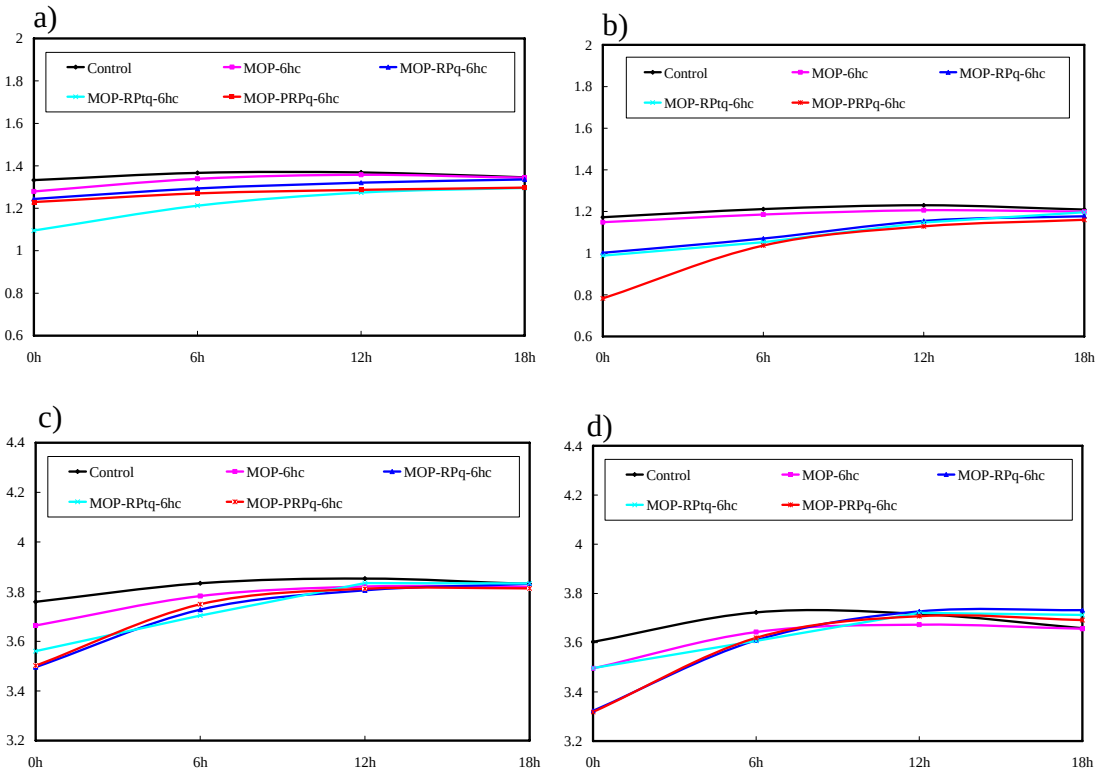

Fig. 22. RMS error as a function of forecast length, averaged over 16 forecasts, for a) temperature *T* (K), b) water vapor mixing ratio *q* (g/kg), c) zonal wind component *u* (m/s), and d) meridional wind component *v* (m/s).

Figure 23 compares the 18-h accumulated precipitation at 12UTC 12 June 2002 in the control, MOP, MOP-RPq-6hc and MOP-RPtq-6hc experiments with the nature run. The control experiment under-predicts the heavy precipitation. Assimilating conventional observations (MOP) and MTG-IRS retrievals intensifies the precipitation in the heavy rainfall region. However, it also produces spurious light rainfall in the southern states.

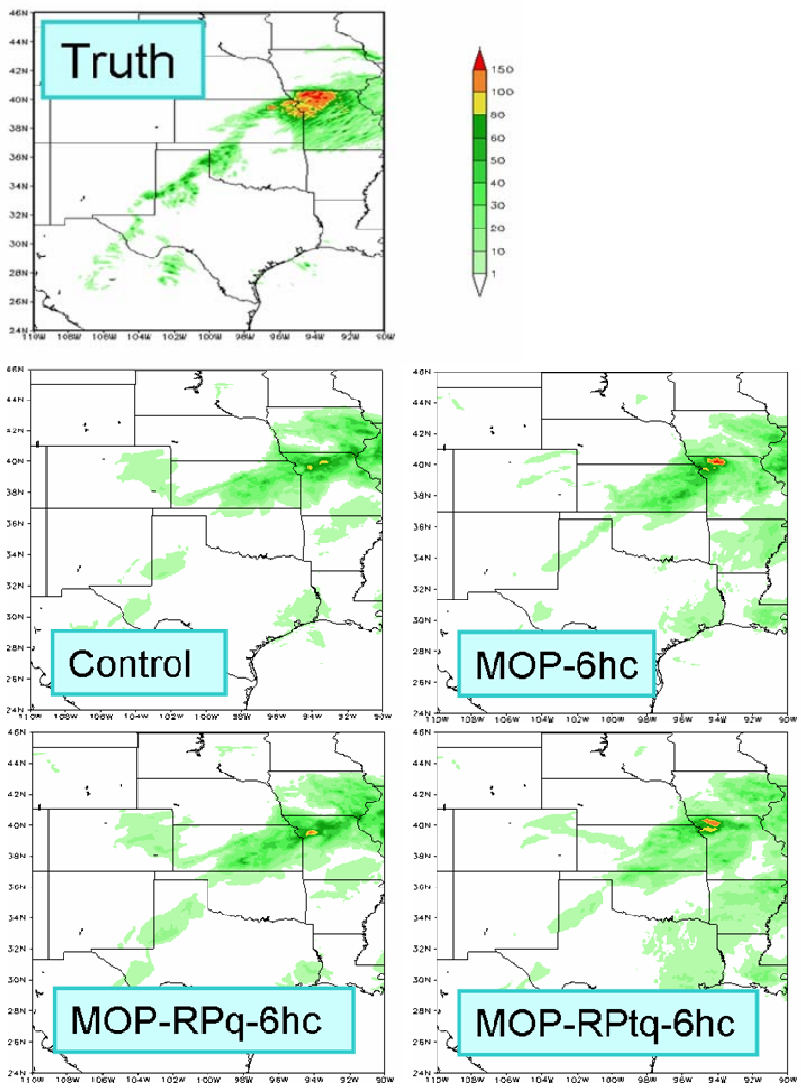

Fig. 23. 18-h accumulated precipitation (mm) valid at 12UTC 12 June 2002.

The equitable threat scores for 18-h accumulated rainfall with thresholds of 10 mm, 30 mm, 50 mm, 65 mm, 80 mm and 100 mm are shown in Fig. 24. It is evident that assimilating MTG-IRS retrievals substantially improves precipitation forecast skill with threshold larger than 50 mm, but degrades slightly the precipitation prediction skill with threshold smaller than 30 mm for this case. The rainfall forecast frequency for experiments MOP-RPtq-6hc, and MOP-RPq-6hc is lower than experiments MOP with threshold larger than 30 mm.

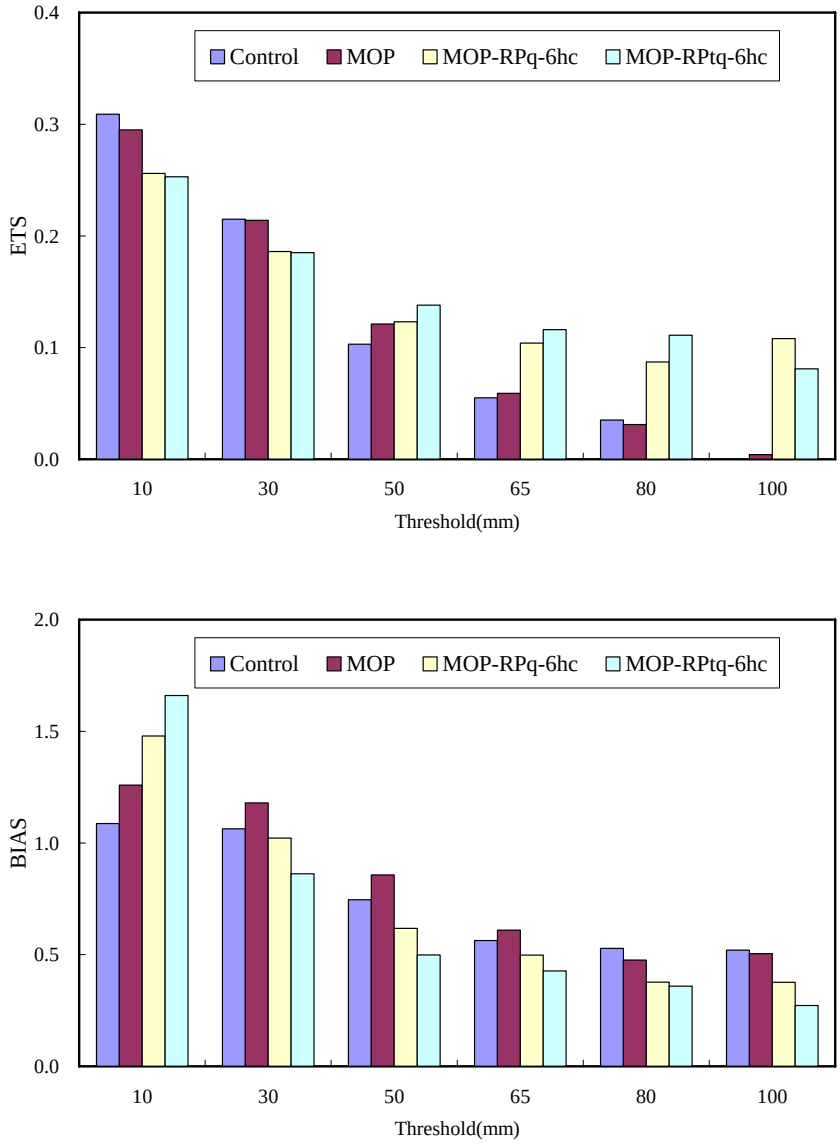

Fig.24. ETS (up panel) and BIAS (bottom) of 18-h accumulated precipitation for experiments Control, MOP, MOP-RPtq-6hc, and MOP-RPq-6hc, valid at 12 UTC 12 June, 2002.

For the second convective event, the 18-h accumulated precipitation at 12UTC 13 June 2002 in different experiments is shown in Fig. 25. The equitable threat scores for 18-h accumulated rainfall with thresholds of 10 mm, 30 mm, 50 mm, 65 mm and 80 mm are shown in Fig. 26. In this case, MTG-IRS humidity retrievals (MOP-RPq-6hc) have positive impacts on precipitation forecast with threshold larger than 30 mm; MTG-IRS temperature and humidity retrievals (MOP-RPtq-6hc) help to improve precipitation forecast skill with threshold smaller than 30 mm. The rainfall forecast frequency for

experiments MOP-RPtq-6hc, and MOP-RPq-6hc is higher than experiments MOP with threshold larger than 30 mm.

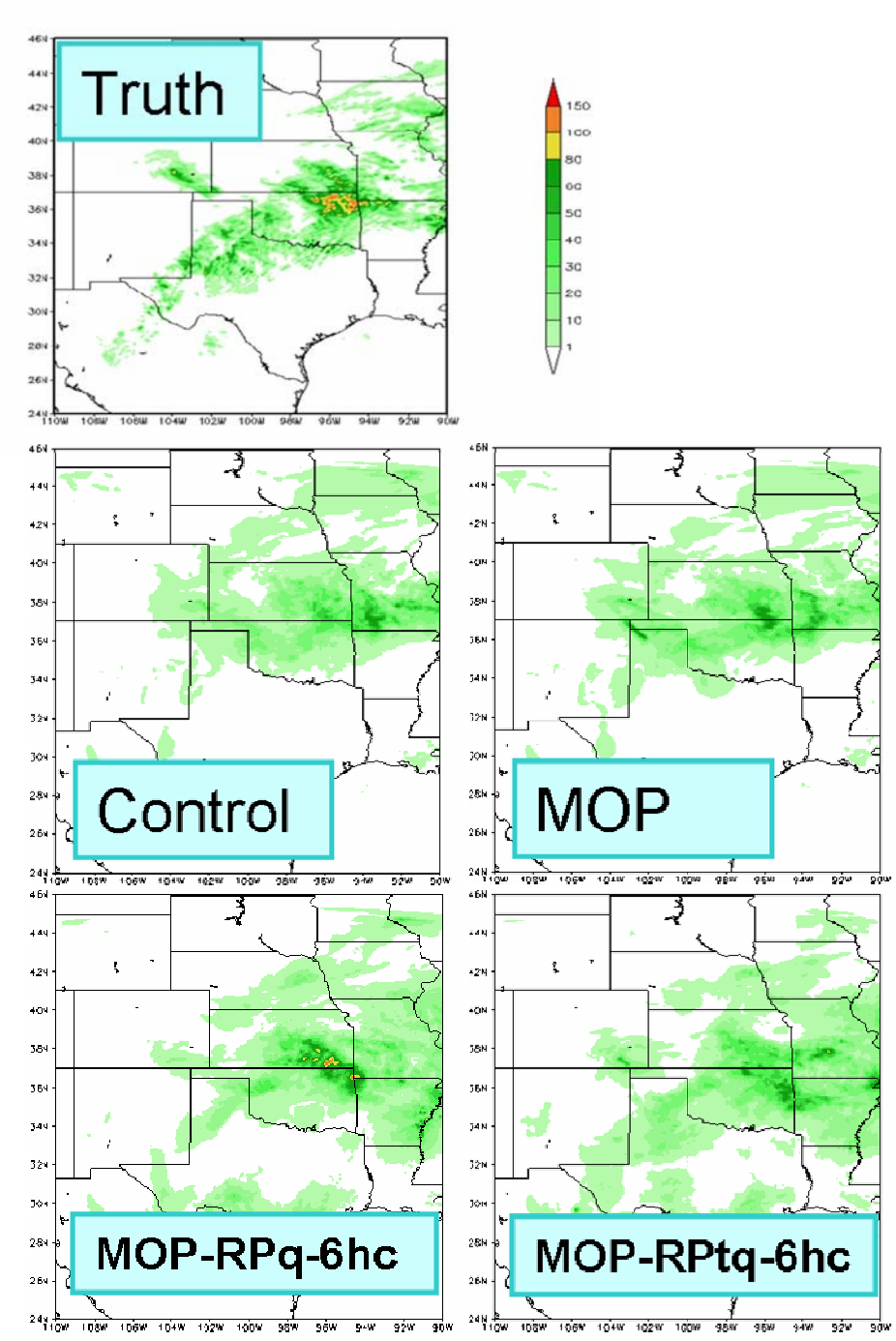

Fig.25. 18-h accumulated precipitation (mm) valid at 12UTC 13 June 2002.

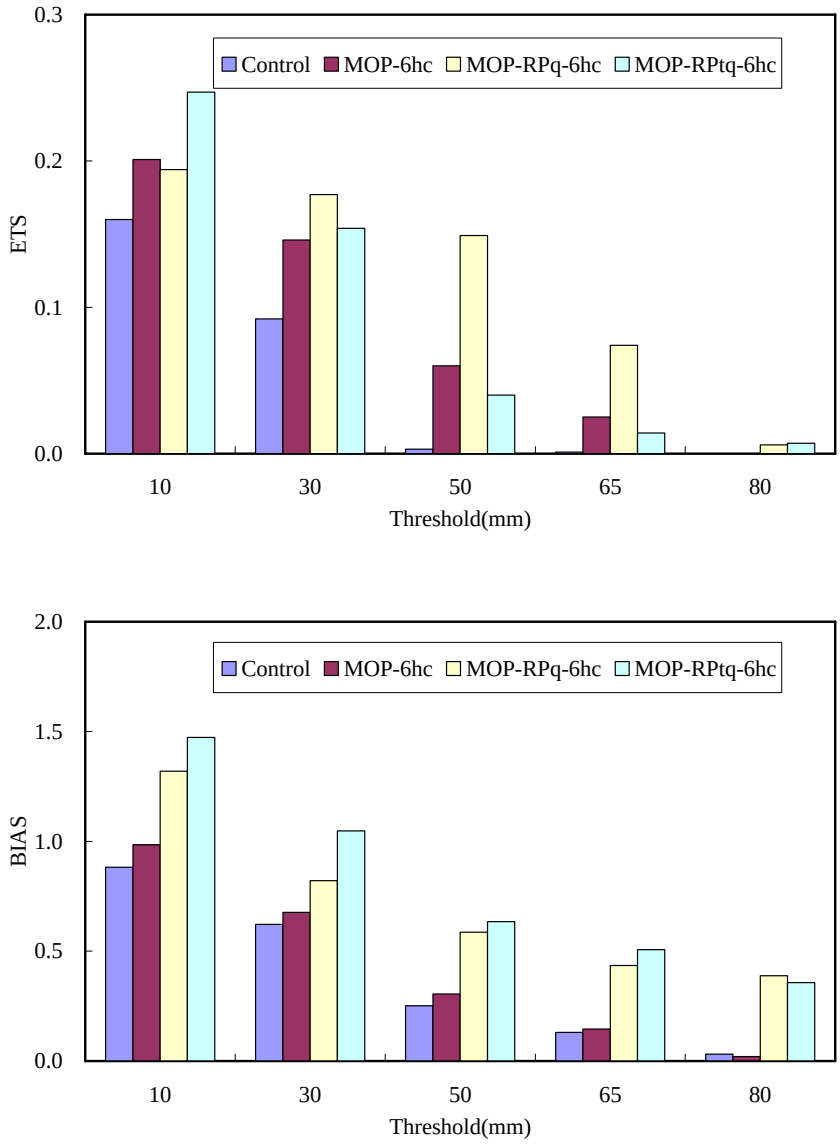

Fig.26. ETS (up panel) and BIAS (bottom) of 18-h accumulated precipitation for experiments Control, MOP, MOP-RPtq-6hc, and MOP-RPq-6hc.

Over the cycling period, 12 analyses and forecasts are made. The averaged equitable threat scores and bias of these 12 forecasts are shown in Fig. 27 and Fig.28 respectively. On average, assimilating MTG-IRS retrievals leads to better ETS of rainfall forecast with threshold larger than (including) 30 mm. MTG-IRS humidity retrievals (MOP-RPq-6hc) have slightly positive impacts on precipitation forecast with threshold larger than 30 mm as well.

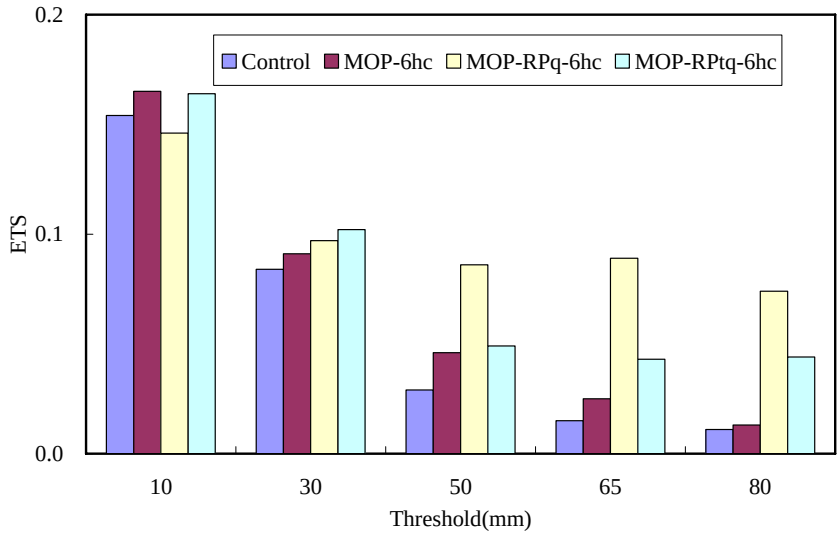

Fig.27. The averaged equitable threat score of 18-h accumulated precipitation for all experiments of 12 forecasts

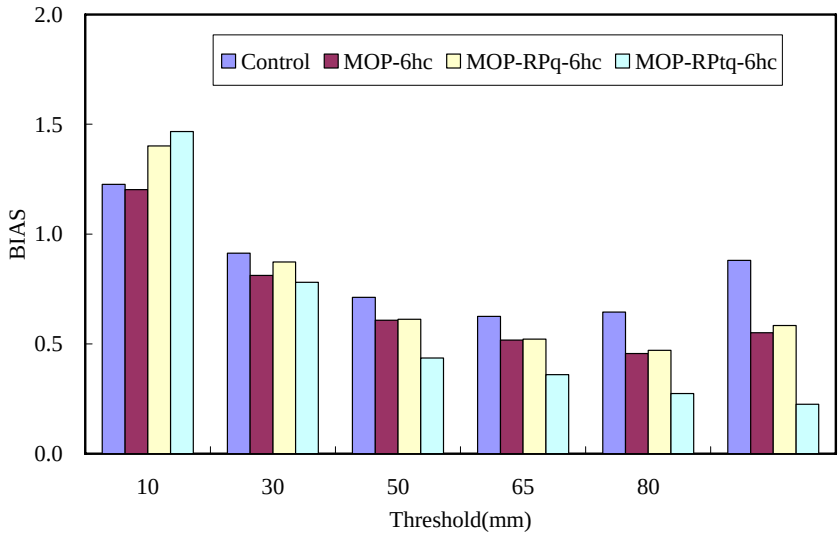

Fig.28. The averaged BIAS of 18-h accumulated precipitation for all experiments of 12 forecasts

4.6 ***Analysis and forecast in 3 and 1 hourly cycling experiments***

Since high temporal resolution MTG-IRS retrievals can be obtained, it is interesting to test their impact on the regional forecast. Three 3-hourly cycling and a 1-hourly cycling experiments have been carried out. Increasing assimilation frequency, however, has only neutral or even negative impacts on the analysis and forecast comparing to 6-hourly

cycling experiments. In the experiments MOP-RPtq-3hc, MOP-RPq-3hc and MOP-RPq-1hc, we found that when the MTG-IRS retrievals are assimilated, the horizontal wind analyses are degraded, which leads to degraded forecast and subsequent analysis. This could be due to the lack of upper air wind observation at asynoptic times. The fact that a few upper air wind observations available every 6 hours can bring back improved wind analysis at the synoptic time suggests that more frequent wind observations are necessary to make the best use of MTG-IRS in our 3D-Var system. We propose to test our hypothesis by assimilating more wind observations such as those from the simulated wind profilers.

5 Summary

To document the added value of water vapor observations derived from an IRS sounding instrument on a geostationary satellite to the existing conventional observing system for regional forecasting, a set of OSSE's is designed. Three cases covering dryline, convective storms and MCS are selected for this study.

The 5 day 4-km high-resolution nature runs of three cases have been completed using MM5. The model reproduces the reality quite well. The 12km resolution data assimilation experiments of two cases occurred on 11-13 June 2002 are conducted.

The MTG-IRS retrieved temperature and moisture fields over the clear sky region are compared against the nature run. It is found that the retrievals recover the large scale and some mesoscale temperature and moisture variations. The retrieval error in temperature is very small (less than 1 K). The humidity retrieval near surface has errors as large as 2 g/kg.

The results of 6-hourly cycling data assimilation and forecast experiments show that the assimilation of MTG-IRS retrievals has positive impacts on the forecast. The forecast skills for T, q, u and v are improved. The quantitative precipitation forecasts are also improved, in particular for heavy precipitation events.

In the 3-hourly and 1-hourly cycling experiments, assimilating frequent MTG-IRS temperature and moisture observations has only neutral or negative impacts on the analysis and forecast. Further studies are needed to understand the problem. As assimilating temperature information sometimes leads to degradation of wind analysis, tuning of the background error will be carried out. Introducing some additional hourly wind observations will also be tested.

References

Barker, D.M., J. Bray, Y.-R. Guo, X.-Y. Huang, Z. Liu, S. Rizvi, Q.-N. Xiao, 2006. Status Report on WRF-ARW's Variational Data Assimilation System (WRF-Var). WRF users' workshop, Boulder, Colorado, 19-22 June 2006.

Cai, H.Q., LEE, W.C, Weckwerth, T. M et al., 2006: Observations of the 11 June Dryline during IHOP_2002—A Null Case for Convection Initiation, *Mon. Wea. Rew*, **134,** 336-354

Chen, F., and J. Dudhia, 2001: Coupling an advanced land-surface/ hydrology model with the Penn State/ NCAR MM5 modeling system. Part I: Model description and implementation. *Mon. Wea. Rev.*, 129, 569–585.

Chen, S.-H., and W.-Y. Sun, 2002: A one-dimensional time dependent cloud model. *J. Meteor. Soc. Japan*, 80, 99–118.

Crook, N. A., 1996: Sensitivity of moist convection forced by boundary layer processes to low-level thermodynamic fields. *Mon. Wea. Rev.*, **124,** 1768–1785.

Dawson II, D.T, Xue, M, 2006, Numerical Forecasts of the 15–16 June 2002 Southern Plains Mesoscale Convective System: Impact of Mesoscale Data and Cloud Analysis. *Mon. Wea. Rew*, **134,** 1607-1629.

Dudhia, J., 1993: A nonhydrostatic version of the Penn State/NCAR Mesoscale Model: Validation tests and simulation of an Atlantic cyclone and cold front. *Mon. Wea. Rev.*, **121**, 1493-1513.

Grell, G. A., and D. Devenyi, 2002: A generalized approach to parameterizing convection combining ensemble and data assimilation techniques. *Geophys Res. Lett.*, **29(14)**, Article 1693.

Hong, S.-Y., and H.-L. Pan, 1996: Nonlocal boundary layer vertical diffusion in a medium-range forecast model, *Mon. Wea. Rev.*, 124, 2322–2339.

Huang, X.-Y., H. Wang, and X. Zhang, 2007a: Benefit of the MTG candidate Infra-Red Sounding mission to regional forecast. Report TN-2: Preliminary results review. MEMETSAT MTG-IRS OSSE project report.

Huang, X.-Y., Q. Xiao, Xin Zhang, J. Michalakes, W. Huang, D.M. Barker, J. Bray, Z. Ma, T. Henderson, J. Dudhia, Xiaoyan Zhang, D.-J. Won, Y. Chen, Y.-R. Guo, H.C. Lin, Y.-H. Kuo. 2007b. 4-Dimensional Variational Data Assimilation for the Weather Research and Forecasting Model. 22nd Conference on Weather Analysis and Forecasting/18th Conference on Numerical Weather Prediction, Park City, Utah, 25-29 June 2007. [http://ams.confex.com/ams/pdfpapers/123878.pdf]

Koch, S. E., A. Aksakal, and J. T. McQueen, 1997: The influence of mesoscale humidity and evapotranspiration fields on a model forecast of a cold-frontal squall line. *Mon. Wea. Rev.*, **125,** 384–409.

Lin, Y.-L., R. D. Farley, and H. D. Orville, 1983: Bulk parameterization of the snow field in a cloud model. *J. Climate Appl. Meteor.*, 22, 1065–1092.

Markowski, P, Hanon, C, Rasmusen, E, 2006: Observations of Convection Initiation

"Failure" from the 12 June 2002 IHOP Deployment. *Mon. Wea. Rew*, **134,** 375-405

Mellor, G. L., and T. Yamada, 1982: Development of a turbulence closure model for geophysical fluid problems. *Rev. Geophys. Space Phys.,* **20,** 851–875.

Michalakes, J., Loft, R., Bourgeois, A., 2001: Performance-Portability and the Weather Research and Forecast Model. *HPC Asia 2001*, doi: ISBN: 0-9579303-0-5.

Michalakes, J., Dudhia, J., Gill, D., Henderson, T., Klemp, J., Skamarock, W., Wang, W., 2004: The Weather Research and Forecast Model: Software architecture and performance. *11th Workshop on High Performance Computing in Meteorology*, 156-168.

Parsons, D. B., M.A.Shapiro.,and E. Miller, 2000: The mesoscale structure of a nocturnal dryline and of a frontal-dryline merger. *Mon. Wea. Rev.,* **128,** 3824–3838.

Reisner, J., R. J. Rasmussen, and R. T. Bruintjes, 1998: Explicit forecasting of supercooled liquid water in winter storms using MM5 Mesoscale Model. *Quart. J. Roy. Meteor. Soc.*, **124B**, 1071-1107.

Skamarock, W. C., J. B. Klemp, J. Dudhia, D. O. Gill, D. M. Barker, W. Wang, and J. G. Powers, 2005: A Description Of The Advanced Research WRF Version. NCAR Tech Note, NCAR/TN-468+STR, 88 pp. [Available from UCAR Communications, P.O. Box 3000, Boulder, CO, 80307.]

Tjemkes, S. 2007 : EUMETSAT MTG-IRS retrieval.

Weckwerth, T. M., 2000: The effect of small-scale moisture variability on thunderstorm initiation. *Mon. Wea. Rev.,* **128,** 4017–4030.

Weckwerth, T. M., and Coauthors, 2004: An overview of the International H2O Project (IHOP_2002) and some preliminary highlights. *Bull. Amer. Meteor. Soc.,* **85,** 253–277.

Xue, M., and W. J. Martin, 2006: A high-resolution modeling study of the 24 May 2002 dryline case during IHOP. Part II: Horizontal convective rolls and convective initiation. *Mon. Wea. Rev.,* **134,** 172–191